Localization and protein-protein interactions of protein kinase CK2 suggest a chaperone-like activity is integral to its function in *M. oryzae*

Lianhu Zhang[1*], Dongmei Zhang[1*], Yunyun Chen[1], Wenyu Ye[2], Qingyun Lin[2], Guodong Lu[1], Daniel J. Ebbole[1,3], Stefan Olsson[1,4,§] & Zonghua Wang[1,2,5§]

[1]*State Key Laboratory for Ecological Pest Control of Fujian and Taiwan Crops, College of Plant Protection, Fujian Agriculture and Forestry University, Fuzhou 350002, China.*
[2]*College of Life Sciences, Fujian Agriculture and Forestry University, Fuzhou 350002, China.*
[3]*Department of Plant Pathology and Microbiology, Texas A&M University, College Station, Texas 77843, U.S.A.*
[4]*Plant Immunity Center, Haixia Institute of Science and Technology, Fujian Agriculture and Forestry University, Fuzhou 350002, China.*
[5]*Minjing University, Fuzhou 350018, China.*

*These authors contributed equally to this work

§ These authors jointly supervised the work

Abstract

CK2 is a constitutively active conserved serine/threonine kinase in eukaryotes. We characterized three components of the CK2 holoenzyme, CKa, CKb1 and CKb2, in the fungus *Magnaporthe oryzae*. The CKa encoding gene appears to be essential. All three CK2 components were localized with GFP fusions and both CKb components were needed for preferential cellular localization to the nucleolus and as structures at septal pores. A unique CK2 filament was prominent within appressoria. A pulldown experiment identified CKa interacting proteins with an overrepresentation of intrinsically unfolded proteins containing a CK2 phosphorylation motif for destabilizing and unfolding alpha helixes. This suggests a role for CK2 in forming protein aggregates. Supporting this conclusion, we found that *CKa* expression and a key autophagy gene, *Atg8,* are strongly correlated, indicating that an increased removal of aggregates is needed with higher CKa expression.

Introduction

Since its discovery (Meggio & Pinna, 2003), the constitutive activity of CK2 and the increasing number of proteins it has been shown to phosphorylate have puzzled scientists (Ahmad, Wang, Unger, Slaton, & Ahmed, 2008; Götz & Montenarh, 2016; Meggio & Pinna, 2003). Indeed CK2 has been implicated in a wide range of cellular processes (Götz & Montenarh, 2016). The CK2 holoenzyme is a heterotetrameric structure consisting of 2 catalytic α-units and 2 regulatory β-subunits (Ahmad et al., 2008). In mammals, there exist two different alpha subunits α (a1) and α' (a2) and the enzyme can contain any combination of α-subunits (α1α1, α1α2, α2α2) combined with the β-subunits. In *Saccharomyces cerevisiae*, CK2 contains two different alpha- and two different β-subunits (b1 and b2) (Padmanabha, Chen-Wu, Arnot, & Glover, 1990). CK2 has been extensively studied in the budding yeast *S. cerevisiae* (Padmanabha et al., 1990), however, functions of CK2 involved in multicellularity might be obscured in yeast. For fungi, it has been reported that deletion of both catalytic subunits is lethal (Padmanabha et al., 1990; C. Wang et al., 2011) and some fungi, including *M. oryzae*, contain only one gene encoding CKa (Mehra et al., 2009). In comparison to yeast, filamentous fungi have different cell types that allow detailed exploration of cellular differentiation and multicellular development (Shlezinger, Goldfinger, & Sharon, 2012) and this, in combination with haploid life-cycles, well characterized genomes, and efficient methods for targeted gene replacement, makes fungi like *Magnaporthe oryzae* and *F. graminearum* good model systems for molecular studies of basic eukaryote functions including cell-cell communication (Cavinder, Sikhakolli, Fellows, & Trail, 2012; Ebbole, 2007). As plant pathogens, developmental processes needed for symbiosis can also be explored. We focused our study on *M. oryzae* one of the most important rice crop pathogens worldwide (Dean et al., 2012).

Our results show that *M. oryzae* CK2 holoenzyme (MoCK2) accumulates in the nucleolus, localizes in structures near septal pores, and assembles to form a large ring structure perpendicular to the appressorium penetration pore, which we call the CK2-Holoenzyme Ring Structure (CK2-HRS). The large-scale structures formed by CK2 protein kinase, combined with our finding of the interaction of CK2 with substrates associated with the location of CK2 enzyme aggregation, suggests that CK2 may control substrate stability and localization near their sites of action. Furthermore, CK2 interacts preferentially with proteins annotated as being intrinsically disordered. Taken together, this work provides further evidence supporting the view that one of the roles for the CK2 holoenzyme is to induce conformational changes in intrinsically disordered proteins.

RESULTS

Deletion of MoCK2 components

Using BLASTp and the protein sequences for the CK2 catalytic subunits of *S. cerevisiae,* CKa and CKa2 (encoded by *CKA1* and *CKA2*), and CKb1 and CKb2 (encoded by *CKB1* and *CKB2*) (Padmanabha et al., 1990), we identified one MoCKa (MGG_03696) and two MoCKb sequences (MoCKb1 = MGG_00446, MoCKb2 = MGG_05651) (Figure 1). Sequence alignments and phylogenetic analysis show that these proteins are highly conserved in different fungi (Figure 1 Supplement 1-4). Moreover, the phylogenetic analysis indicated that the two CKbs were in two separate evolutionary branches (Figure 1 Supplement 1).

We attempted targeted deletions of the three identified genes and succeeded in deleting the two *CKb* genes but not the *CKa* and then also saw that the conidial

morphology was different in the CKb mutants in that they had lower numbers of conidial compartments (Figure 2).

Subcellular localization of CK2 subunits

To assess the localization of the three CK2 subunit mutants, we constructed GFP fusions of all three proteins (Filhol et al., 2003) (GFP-MoCKa, GFP-MoCKb1 and GFP-MoCKb2) (Table 1). All three strains showed the same growth, morphology and pathogenicity (Figure 3) as the background strain Ku80. The CKa and CKb1&2 fusion proteins localized to nuclei and prominently to nucleoli and, interestingly, to both sides of septal pores in hyphae (Figure 4 a-e) and conidia (Figure 4 Supplement 1). We then tested if the localization to septa and nucleoli were dependent on the association with the other subunits of the holoenzyme. We had measured MoCka expression in the two *MoCkb* mutants using qPCR and noted it was downregulated compared to the background strain Ku80 (Figure 5 a). Thus, we constructed strains that over-express GFP-CKa in the *ΔMockb1* and *ΔMockb2* deletion strains (43OE and 53OE respectively, Figure 5 b-e) but this did not result in localization to septa (Figure 4 f,g). However, Nucleolar localization of GFP-MoCKa was clear even in the *MoCKb1* and *MoCKb2* mutant backgrounds. To test if over-expression of any one of the CKb proteins could rescue the effect of the deletion of the other CKb we constructed GFP-CKb overexpression strains in the background strain Ku80 and both CKb mutants, GFP-CKb1 in *ΔMockb2* (54OE-GFP) and GFP-CKb2 in *ΔMockb1* (45OE-GFP). The overexpression of either of the two CKbs in the background strain Ku80 showed normal localization to septa and nucleolus but the overexpression in the deletion strains could not rescue normal localization (Figure 4h,i and Figure 5 Supplement 1). Furthermore, GFP-MoCKb1 appeared to localize to nuclei but not nucleoli in the *MoCKb2* mutant. Similarly, GFP-MoCKb2 also appeared to localize

to nuclei but not nucleoli in the *MoCKb1* mutant. Conidia morphology also changed in the *ΔMockb2* deletion mutants (Figure 2c), even if CKa was overexpressed as in 43OE and 53OE (Figure 5), which restored some of the conidia formation and growth rate defects (Figure 5). These conidia mainly contained 2 nuclei instead of the normal 3 found in the background strain Ku80 (Figure 2c, Figure 5 d,e). Compared to the background strain Ku80, all mutants lacking one of the MoCK2b components had severely reduced or absent pathogenicity even if other MoCK2 components were over-expressed.

Infection phenotypes of CKb deletions

Deletion of CK2 genes has been shown to have effects on both growth and infection in *Fusarium* (Wang et al., 2011) and we also found this to be the case for *M. oryzae* (Figure 6 and Figure 6 Supplement 1). Conidiation was very limited or absent in *ΔMockb1* and *ΔMockb2* deletion mutants thus we used mycelia plugs to test for infection (W. Liu et al., 2010; Talbot et al., 1996), and found that infection was strongly reduced or completely absent (Figure 6c).

CKa localization in appressoria

Since we found large effects in infection of the deletion of the CKb components we decided to investigate localization of CKa-GFP in the appressoria of the background strain Ku80 and the two CKb deletion mutants. Normal appressoria were only formed in the background strain Ku80 and in these, CK2 localizes to nuclei (Figure 7a top row and Figure 7 Supplement 1b), to the septa between the appressorium and the germ tube (Figure 7 Supplement 1) and also assembles a large ring structure perpendicular to the penetration pore (Figure 7 b-d, Figure 7 Supplement 1, Figure 7

Supplement 2 for ring size measurements, and movies associated with the images of Figure 7b-d, showing 3D rotations to visualize ring and the appressoria). MoCKa nuclear localization was present but ring structures were absent in appressoria formed by the two CK2b deletion mutants (Figure 7a middle and bottom row). As can be seen in Figure 7d, the CK2 Holoenzyme Ring Structure (CK2-HRS) is positioned perpendicular to the penetration pore where the F-actin-septin ring has been shown to form around the pore opening (Dagdas et al., 2012) (Figure 7d and 8 schematic drawing).

Identification of potential septal and nucleolar substrates for MoCK2 by GFP-CKa pulldown

The localization pattern suggested that CK2 may have substrates associated with septa and nucleolar function. To explore this, we performed co-immunoprecipitation to identify proteins interacting with CK2 using GFP-CKa as a "bait", and in addition to the bait, identified 1505 proteins (Supplementary File 1). We also searched the *M. oryzae* proteome for proteins containing the CK2 phosphorylation helix unfolding motif identified by Zetina (Zetina, 2001) using the FIMO tool at the MEMEsuit website (http://meme-suite.org/) and found 1465 proteins (Supplementary File 2) with the motif, out of a total of 12827 proteins annotated for *M. oryzae.*

There is the risk of false positives in the pulldown. We estimated the number of false positives and removed 155 (10%) of the lower abundance proteins to arrive at a list of 1350 CKa interacting proteins (see Methods). We found 275 of these proteins contain at least one unfolding motif for alpha helixes. Thus, there is an overrepresentation of the motif among the pulldown proteins (Supplementary File 2) (P-value for the null hypothesis of same frequency as in the whole proteome = 4 E-19, Fisher's Exact test) lending support for the proposed role for this motif as a target for CK2

phosphorylation and protein unfolding. As expected, the pulldown caught both CKb proteins.

Since CK2 locates to septa we looked for known septal proteins in the pulldown. All previously proteins identified by Dagas et al. (Dagdas et al., 2012) that are involved in appressorium pore development, were found in the pulldown as was a protein annotated as the main Woronin body protein, Hex1 (MGG_02696). Since the Woronin body in Ascomycetes is tethered to the septal rim by Lah protein (Han, Jin, Maruyama, & Kitamoto, 2014; Ng, Liu, Lai, Low, & Jedd, 2009; Plamann, 2009) we searched for a homologue in *M. oryzae* and found a putative MoLah (MGG_01625) with a similar structure as in *Aspergillus* (Han et al., 2014) that is also present in the pulldown. In addition to the Lah, 18 other intrinsically disordered septal pore associated proteins (Spa) were described for *Neurospora crassa* (Lai et al., 2012). We identified putative orthologs for 15 of the 18 Spa proteins in *M. oryzae* (Supplementary File 3). Of these putative MoSpa proteins, six were present in the CKa pulldown, Spa3 (MGG_02701), Spa5 (MGG_13498), Spa7 (MGG_15285), Spa11 (MGG_16445), Spa14 (MGG_03714) and Spa 15 (MGG_15226). Spa3, Spa5 and Spa15 also contain the CK2 phosphorylation alpha helix unfolding motif (Supplementary File 1).

To further test the hypothesis that CK2 could interact with and possibly phosphorylate intrinsically unfolded proteins we used the FuncatDB (http://mips.helmholtz-muenchen.de/funcatDB/) to make a functional classification of the pulldown proteins including those containing the alpha helix unfolding motif (Zetina, 2001). We found strong overrepresentation for proteins involved in rRNA processing among the pulldown proteins containing the alpha helix unfolding motif as well as for proteins that bind to other proteins, DNA, and RNA (Supplementary File 4). These classes of proteins are enriched for intrinsically disordered proteins that can help create membraneless organelles, such as nucleoli (Wright & Dyson, 2015).

Since CK2 localizes to the nucleolus we were especially interested in the interaction of CK2 with nucleolar localized proteins. We identified homologues to the well described *S. cerevisiae* nucleolar proteins and found a total of 192 proteins in *M. oryzae* homologous to yeast nucleolar proteins (Supplementary File 5). We found 120 (63%) of the nucleolar proteins in the pulldown and 60 of these (50%) had the alpha helix unfolding motif (Supplementary File 1 and 4). The nucleolar proteins were highly overrepresented in the pulldown (P-value for the null hypothesis of same frequency as in the whole proteome 9E-43 Fisher's Exact test) (Supplementary File 5) compared to the whole proteome as was also nucleolar proteins having the unfolding motif (P-value for the null hypothesis of same frequency as in the whole proteome 2E-13 Fisher's Exact test) (Supplementary File 5).

Interestingly the pulldown proteins without the unfolding motif were strongly enriched (60 of 130 in the whole proteome, P-value for the null hypothesis of same frequency as in the whole proteome 1.0E-29) for proteins that are imported into mitochondria and involved in oxidative phosphorylation ("02.11 electron transport and membrane-associated energy conservation" category from Funcat) (Supplementary File 4).

There was however no enrichment for specific pathogenicity related proteins and rather an underrepresentation of pathogenicity related proteins (Funcat category 32.05 disease, virulence and defence) (Supplementary File 4) and within the whole Funcat category related to stress and defence (32 CELL RESCUE, DEFENSE AND VIRULENCE). The lack of association of pathogenicity related proteins with CK2 may reflect the in vitro growth conditions of the experiment where pathogenicity related proteins would either not be expressed or not active. There was a considerable overrepresentation for proteins involved in the unfolded protein response (32.01.07 unfolded protein response) (e.g. ER quality control) which is

notable since an involvement of CK2 in protein import into the ER has be established (X. Wang & Johnsson, 2005).

Interestingly five putative S/T phosphatases (MGG_03154, MGG_10195, MGG_00149, MGG_03838, MGG_06099) were in the pulldown set of proteins (Supplementary File 1). Conceivably these might de-phosphorylate CKa substrates as well as substrates of other kinases to expand the reach of CK2 in regulating the phosphoproteome. If that idea is correct, increased CK2 activity should also be followed by an increased activity of the phosphatases that dephosphorylate the proteins CK2 has phosphorylated. Thus, the expression of the phosphatases involved can be expected to be transcriptionally co-regulated with CKa. To evaluate this possibility, we downloaded expression data from a range of experiments with *M. oryzae* and plotted the expression of the phosphatases as a function of the CKa expression and found that two of the S/T phosphatases present in the pulldown were strongly correlated CKa (Figure 9).

CK2 expression correlates with autophagy

Since CK2 activity has the potential to favour protein-protein binding between intrinsically disordered proteins it consequently also has the potential to enhance protein aggregate formation of "garbage" that needs to be degraded through autophagy since these kinds of aggregates are too big for proteasome degradation (Wong & Cuervo, 2010). If this is the case CK2 upregulation should be accompanied by higher autophagy flux or at least there should not be low expression of key autophagy genes when CK2 expression is high (Wong & Cuervo, 2010). To test this hypothesis, we used the expression data we downloaded for *M. oryzae* and also for another fungal plant pathogen, *Fusarium graminearum*, that has rich transcriptomic data available (see methods).

For both fungi we plotted *CKa* versus *Atg8* expression across experiments. Atg8 is a key autophagy protein for which its turnover rate can reflect autophagy flux (Klionsky et al., 2016). For both *M. oryzae* and *F. graminearum* we find a log-log linear relationship between the CKa expression and Atg8 expression (Figure 9 with Supplements 1 and 2) across a large range of experiments supporting the hypothesis that autophagy activity is increasingly needed to remove protein aggregates stimulated to form by increasing levels of CKa and its activity in the cell.

Discussion

In contrast to *S. cerevisiae* (Padmanabha et al., 1990) and *F. graminearum* (C. Wang et al., 2011) but consistent with *N. crassa* (Mehra et al., 2009) we only found one CKa encoding gene in *M. oryzae*. In fungi where two different *CKa* genes are found deletion of both is lethal (Padmanabha et al., 1990; C. Wang et al., 2011), so it is rather expected that we were not able to obtain a *ΔMocka* mutant.

The analysis of the *MoCKb* mutants and the localization of the GFP-labelled MoCK2 proteins showed that all identified MoCK2 components are needed for normal function and also normal localization. Localization to septa requires all three subunits, presumably as the holoenzyme. Mutation of either CKb subunit blocks nucleolar localization of the other CKb subunit. Surprisingly, nucleolar localization of CKa was observed in the CKb mutants. This shows that the holoenzyme is not required for CKa localization to the nucleolus. It seems likely that CKb1 and CKb2 must interact with each other in order to interact with CKa, and that CKa is required for movement of CKb subunits into the nucleolus as the holoenzyme.

The pattern of localization to septa (Figures 4) observed is remarkably similar to that displayed by the Woronin body tethering protein AoLah from *Aspergillus oryzae* (Figure 4b in (Han et al., 2014)). Pulldown experiments demonstrate that CK2

interacts with proteins that function in septum formation and function, including the MoLah ortholog, supporting the view that localization of the GFP-fusion proteins gives a proper representation of CK2 localization. Our results thus demonstrate that the MoCK2-holoenzyme assembles as a large complex near, and is perhaps tethered to, septa, possibly through binding to MoLah. Since septal pores in fungi are gated (Shen K-F., Osmani A. S., Govindaraghavan M., & Osmani S. A., 2014), as are gap junctions and plasmodesmata in animal and plant tissue, respectively (Ariazi et al., 2017; Kragler, 2013; Neijssen et al., 2005), CK2 has a potential to play a general role in this gating.

The crystal structure suggested that CK2 can form filaments and higher-order interactions between CK2 holoenzyme tetramer units, and based on this it has been predicted that autophosphorylation between the units could occur to down-regulate activity (Litchfield, 2003; Poole et al., 2005). Filament formation has been shown to occur *in vitro* (Glover, 1986; Seetoh, Chan, Matak-Vinković, & Abell, 2016; Valero et al., 1995) and in vivo (Hübner et al., 2014). Several forms of higher order interactions have been predicted, and it has been demonstrated that at least one of these has reduced kinase activity (Poole et al., 2005; Valero et al., 1995). However, in our localization experiments we cannot distinguish if the large structure is due to co-localization of the CK2 with another protein, such as the MoLah ortholog, or if CK2 is in an aggregated form near septa. Since MoLah has the characteristics of an intrinsically disordered protein (Han et al., 2014), and CK2 interacts with some proteins to favour their disordered state, we favour the view that CK2 interacts with MoLah and other proteins to form a complex near septa.

Our pulldown experiment with GFP-CKa further showed that there was a strong overrepresentation of proteins interacting with CKa that contain known

phosphorylation motifs for unfolding of alpha-helixes and this is what would be expected for intrinsically disordered proteins (Uversky, 2015; Zetina, 2001). The finding of overrepresentation of this signal in the set of CK2 interacting proteins corroborates the previous suggestion that CK2 is involved in the destabilization/binding of intrinsically disordered proteins (Zetina, 2001) and is consistent with the strong accumulation of both CK2 and intrinsically disordered proteins in the nucleolus (Fig. 4a and b) (Frege & Uversky, 2015) and also at pores between cell compartments (Lai et al., 2012) (Figure 4d). In addition, and further supporting this conclusion, the six septal pore associated proteins (SPA) that we find in the CKa pulldown are homologues for intrinsically disordered proteins that are expected to form temporary gels that are used to reversibly plug septal pores and regulate traffic through septa (Lai et al., 2012), CK2 could actively be involved in the gelling/un-gelling of the regions near septa to create a membraneless organelle controlling the flow through septa.

A close look at the subcytolsolic localization reveals that this enzyme is also associated with cytosolic organelles protein import into organelles. CK2 promotes protein import into endoplasmic reticulum (Wang & Johnsson, 2005) and into mitochondria and mitochondrial biogenesis (Rao et al., 2011). CK2 phosphorylation has been shown to be needed to activate Tom 22 precursors to get a functional mitochondrial import machinery (Rao et al., 2011). Although CK2 has been implicated to be located in mitochondria in earlier works in other organisms no proteomic study of yeast mitochondria has detected a presence of CK2 (Rao et al., 2011) wherefore we do not expect MoCK2 to be present in mitochondria. Of special interest was consequently the strong overrepresentation of mitochondrial proteins among the CKa pulldown proteins without the alpha helix phosphorylation unfolding motif (Supplementary File 4). Since these proteins need to be imported into mitochondria in an unfolded unbound state this may point to the existence of other

CKa phosphorylation and unfolding motifs that help keep these proteins unfolded until they reach their destination inside the mitochondria.

To have such dynamic function as an unfolder of proteins by phosphorylation, CK2 should be partnered with phosphatases as counterparts and their activity may track CK2 activity. Consistent with this possibility, we found that two of the five S/T phosphatases that are present in the pulldown are transcriptionally strongly co-regulated with CKa (Figure 9), further supporting the view that CKa-dependent phosphorylation/dephosphorylation plays a major role in shaping protein interactions. Together with the high expression of CK2 in cells, this suggests an important function of CK2 as a general temporary unfolder of intrinsically disordered proteins that comprise roughly 30 % of eukaryotic proteins (Vucetic, Brown, Dunker, & Obradovic, 2003).

As MoCK2 is present in the cytoplasm and nucleoplasm it could generally assist intrinsically disordered proteins forming larger protein complexes (Uversky, 2015). It also seems to be essential for assembling ribosomes containing large numbers of intrinsically disordered proteins (Uversky, 2015). All these functions also explains why CK2 is needed constitutively (Meggio & Pinna, 2003).

In the absence of well-functioning autophagy removing incorrectly formed larger protein aggregates, like those formed in brain cells of Alzheimer's patients (Zare-shahabadi, Masliah, Johnson, & Rezaei, 2015), CK2 activity facilitates protein aggregate formation and hastens the progression of Alzheimer's disease (Rosenberger et al., 2016). Using publicly available transcriptome datasets we could show that CKa expression in *M. oryzae* and *F. graminearum* is strongly correlated to Atg8 expression (Figure 8), and thus autophagy, giving further support for a relationship of CK2 in facilitating the formation of protein aggregates from intrinsically unfolded proteins that are then subjected to autophagy. As autophagy is important to

appressorium development (X. Liu & Lin, 2008; Kershaw & Talbot, 2009), it will be of interest to further examine the role of the CK2 ring structure during appressorial development and infection. The CK2-HRS may be a true filament of CK2 in a relatively inactive state that may be a store for CK2 so that upon infection, it can facilitate rapid ribosome biogenesis, appressorial pore function, and other pathogenesis-specific functions.

Conclusion

We conclude that CK2 most likely has an important role in the correct assembly/disassembly of intrinsically disordered proteins as well as allowing these proteins to pass through narrow pores between cell compartments in addition to its already suggested role in organelle biogenesis (Rao et al., 2011). Our results further point to one of the main functions of the CK2 holoenzyme as a general facilitator of protein-protein interactions important for a large range of cellular processes including a potential role for gel formation that creates membraneless organelles at septa through its likely interaction with, and modification of, intrinsically disordered proteins. Most of our evidence for these functions of CK2 is, however, indirect and future experiments and methods development will be needed to directly demonstrate the suggested role for CK2 in relation to intrinsically disordered proteins.

Methods

Fungal strains, culture, and transformation

The *M. oryzae* Ku80 mutant (kindly provided by Professor Jin-Rong Xu Department of Botany and Plant Pathology Purdue University, U.S.A.) of the wild type Guy11 strain was used as background strain since it lacks non-homologous end joining which facilitates gene targeting (Villalba et al., 2008). Ku80 and its derivative strains

(Table 1) were all stored on dry sterile filter paper and cultured on complete medium (CM: 0.6% yeast extract, 0.6% casein hydrolysate, 1% sucrose, 1.5% agar) or starch yeast medium (SYM: 0.2% yeast extract, 1% starch, 0.3% sucrose, 1.5% agar) at 25°C. For conidia production, cultures were grown on rice bran medium (1.5% rice bran, 1.5% agar) with constant light at 25°C. Needed genome and proteome FASTA files was downloaded from an FTP-server at the Broad Institute (ftp://ftp.broadinstitute.org/pub/annotation/fungi/magnaporthe/genomes/magnaporthe_oryzae_70-15_8/). Fungal transformants were selected for the appropriate markers inserted by the plasmid vectors. The selective medium contained either 600 μg/ml of hygromycin B or 600 μg/ml of G418 or 50 μg/ml chlorimuron ethyl.

MoCKb gene replacement and complementation

Gene replacement mutants of *MoCKb1* encoding protein MoCKb1 were generated by homologous recombination. Briefly, a fragment about 0.9 Kb just upstream of *Mockb1* ORF was amplified with the primers 446AF and 446AR (Table 2), so was the 0.7Kb fragment just downstream of *Mockb1* ORF amplified with the primers 446BF and 446BR (Table 2). Both fragments were linked with the hygromycin phosphotransferase (*hph*) gene amplified from pCX62 (containing the fragment of TrpC promoter and hygromycin phosphotransferase (*hph*) gene, HPH resistance). Then the fusion fragments were transformed into protoplasts of the background strain Ku80. The positive transformant *ΔMockb1* was picked from a selective agar medium supplemented with 600 μg/ml of hygromycin B and verified by Southern blot.

For complementation of the mutant, fragments of the native promoter and gene coding region were amplified using the primers 446comF and 446comR listed Table 2. This fragment was inserted into the pCB1532 to construct the complementation vector using the XbaI and KpnI. Then this vector was transformed into the

protoplasts of the *ΔMockb1* mutant. The positive complementation transformant MoCKb1C was picked up from the selective agar medium supplemented with 50μg/ml chlorimuron ethyl.

As for the *ΔMoCKb1* deletion mutant, we constructed a knockout vector to delete the *MoCKb2* from the background strain Ku80. All the primers are listed in the Table 2. The 1.0Kb fragment upstream of *MoCKb2* ORF was amplified with the primers 5651AF and 5651AR, inserted into the plasmid pCX62 using the KpnI and EcoRI to get the pCX-5A vector. The 1.0Kb fragment downstream of *Mockb2* ORF was amplified with the primers 5651BR and 5651BR, inserted into the vector pCX-5A using BamHI and XbaI to construct the knockout vector pCX-5D. Then this vector was transformed into the protoplasts of Ku80. The positive transformants were picked up from the selective medium supplemented with the 600 μg/ml hygromycin B. For complementation of the mutant, fragments of the native promoter and gene coding region were amplified using the primers 5651comF and 5651comR listed in the Table 2. This fragment was inserted into pCB1532 to construct the complementation vector using the XbaI and XmaI. Then this vector was transformed into protoplasts of the *ΔMockb2* mutant. The positive complementation transformant MoCKb2C was picked up from the selective agar medium supplemented with 50 μg/ml chlorimuron ethyl.

The construction of localization vectors

In order to detect the localization of MoCK2, we constructed localization vectors. The vector pCB-3696OE containing the RP27 strong promoter was used to detect the localization of GFP-MoCKa. The vector pCB-446OE expressed under RP27 strong promoter was used to detect the localization of GFP-MoCKb1. The vector pCB-5651OE expressed by RP27 strong promoter was used to detect the localization of GFP-MoCKb2.

Analysis of conidial morphology, conidial germination and appressoria formation

Conidia were prepared from cultures grown on 4% rice bran medium. Rice bran medium was prepared by boiling 40g rice bran (can be bought for example through Alibaba.com) in 1L DD-water for 30 minutes. After cooling pH was adjusted from to 6.5 using NaOH and 20 g agar (MDL No MFCD00081288) was added before sterilization by autoclaving (121 ºC for 20 minutes). Conidia morphology was observed using confocal microscopy (Nikon A1^{+}). The Conidial germination and appressoria formation were incubated on hydrophobic microscope cover glass (Beckerman & Ebbole, 1996) (Fisherbrand) under 25℃ in the dark. Conidial germination and appressoria formation were examined at 24 h post-incubation (Beckerman & Ebbole, 1996; Ding et al., 2010).

Pathogenicity assay

Plant infection assays were performed on rice leaves. The rice cultivar used for infection assays was CO39. In short, mycelial plugs were put on detached intact leaves or leaves wounded by a syringe stabbing. These leaves were incubated in the dark for 24h and transferred into constant light and incubated for 5 days to assess pathogenicity (Talbot et al., 1996). For infections using conidial suspensions (1×10^5 conidia/ml in sterile water with 0.02% Tween 20) were sprayed on the rice leaves of 2-week-old seedlings.

RNA extraction and real-time PCR analysis

RNA was extracted with the RNAiso Plus kit (TaKaRa). First strand cDNA was synthesized with the PrimeScript RT reagent Kit with gDNA Eraser (TaKaRa). For quantitative real-time PCR, *MoCKa, MoCKb1*, and *MoCKb2* were amplified with the primers listed in Table 2. β-tubulin (XP_368640) was amplified as an endogenous control. Real-time PCR was performed with the TaKaRa SYBR Premix Ex Taq

(Perfect Real Time) (Takara). The relative expression levels were calculated using the $2^{-\Delta\Delta Ct}$ method (Livak & Schmittgen, 2001).

Pulldown and identification of CKa interacting proteins

Total protein samples were extracted from vegetative mycelia of strain GFP-MoCKa and incubated with anti-GFP beads (Chromotek, Hauppauge, NY, USA) 90 minutes at 4°C with gentle shaking. After a series of washing steps, proteins bound to anti-GFP beads were eluted following the manufacturer's instruction. The eluted proteins were sent to BGI Tech (Shenzhen, Guangdong province, China) and analysed by mass spectrometry for analysis of sequence hits against the *M. oryzae* proteome. The transformant expressing GFP protein only was used as the negative control and the Ku80 was used as Blank control. Data from three biological replicates were analyzed against the background of proteins that were bound non-specifically to the anti-GFP beads in GFP transformant and in WT to get the final gene list of genes that was pulldown with CKa (Supplementary File1).

Estimation of non-specific binding of proteins in the pulldown

We developed two methods to estimate the number of non-specific binding proteins found in the CKa pulldown. The first approach is a chemistry-based reasoning and assumes that the degree of unspecific association to the protein per protein surface area is the same for GFP specific hits and for the CK2 holoenzyme pulled down. Using this technique, we estimate that 44-132 proteins are false positive in the CKa pulldown (all proteins pulled down by GFP-Beads or the Beads already removed from the list) (Supplementary File 1). The Second approach is statistical where we assume that binding of the true interacting proteins to CKa are log-normally distributed related to the abundance of each protein in the pulldown, since the median is low and close to zero and negative amounts are impossible. Using the deviation from the theoretical distribution, with higher than expected amounts of a specific

protein, for the less abundant proteins we estimate that 46-81 proteins found in the CKa pulldown (with controls subtracted) were false positive. The higher number was used to set a conservative threshold for which proteins should be included in the analysis (See Supplementary file S1 for details of both methods).

Finding *M. oryzae* proteins containing the helix unfolding motif

The MEME motif LSDDDXE/SLEEEXD (Zetina, 2001) was used to search through the proteome of *M. oryzae* using the FIMO tool at the MEMEsuite website (http://meme-suite.org/). Results were then downloaded and handled in MS Excel to produce a list of proteins with at least one motif hit (Supplementary File 2)

Analysis of CKa expression in relation to Atg8 expression

For *M. oryzae* transcriptome experiment data was downloaded as sra/fastq files from https://www.ncbi.nlm.nih.gov/geo/ and mapped onto the genome found at http://fungi.ensembl.org/Magnaporthe_oryzae/Info/Index. For *Fusarium graminearum* transcriptomic data was downloaded as FusariumPLEX data for in planta experiments from the PlexDB database (http://www.plexdb.org). For each fungus an expression matrix with the different experiments as columns and gene id as rows were prepared. These matrixes we use as general resources for testing correlation of expression between sets of genes. From these matrixes we used the data needed to plot expression of Atg8 vs CKa for the two fungi. Gene expression data used were from the here identified MoCKa, MoAtg8 (MGG_1062) (Veneault-Fourrey, 2006), FgCKa (FGSG_00677) (C. Wang et al., 2011) and FgAtg8 (FGSG_10740) (Josefsen et al., 2012) genes, respectively. Data from the *M. oryzae* expression matrix was also used for plotting MoCKa expression versus the expression of serine/threonine phosphatases found in the CKa pulldown.

Data availability

The data that support the findings of this study are available from the corresponding authors upon reasonable request.

References

Ahmad, K. A., Wang, G., Unger, G., Slaton, J., & Ahmed, K. (2008). Protein kinase CK2 – A key suppressor of apoptosis. *Advances in Enzyme Regulation*, *48*(1), 179–187. https://doi.org/10.1016/j.advenzreg.2008.04.002

Ariazi, J., Benowitz, A., De Biasi, V., Den Boer, M. L., Cherqui, S., Cui, H., … Zurzolo, C. (2017). Tunneling Nanotubes and Gap Junctions–Their Role in Long-Range Intercellular Communication during Development, Health, and Disease Conditions. *Frontiers in Molecular Neuroscience*, *10*. https://doi.org/10.3389/fnmol.2017.00333

Beckerman, J. L., & Ebbole, D. J. (1996). MPG1, a Gene Encoding a Fungal Hydrophobin of Magnaporthe grisea, Is Involved in Surface Recognition. *MPMI*, *9*(6), 450–456.

Cavinder, B., Sikhakolli, U., Fellows, K. M., & Trail, F. (2012). Sexual Development and Ascospore Discharge in Fusarium graminearum. *Journal of Visualized Experiments*, (61). https://doi.org/10.3791/3895

Dagdas, Y. F., Yoshino, K., Dagdas, G., Ryder, L. S., Bielska, E., Steinberg, G., & Talbot, N. J. (2012). Septin-mediated plant cell invasion by the rice blast fungus, Magnaporthe oryzae. *Science*, *336*, 1590–1594.

Dean, R., Van Kan, J. A. L., Pretorius, Z. A., Hammond-Kosack, K. E., Di Pietro, A., Spanu, P. D., … Foster, G. D. (2012). The Top 10 fungal pathogens in molecular plant pathology: Top 10 fungal pathogens. *Molecular Plant Pathology*, *13*(4), 414–430. https://doi.org/10.1111/j.1364-3703.2011.00783.x

520 Ding, S.-L., Liu, W., Iliuk, A., Ribot, C., Vallet, J., Tao, A., … Xu, J.-R. (2010). The Tig1 Histone
521 Deacetylase Complex Regulates Infectious Growth in the Rice Blast Fungus Magnaporthe
522 oryzae. *THE PLANT CELL ONLINE*, *22*(7), 2495–2508.
523 https://doi.org/10.1105/tpc.110.074302
524 Ebbole, D. J. (2007). Magnaporthe as a Model for Understanding Host-Pathogen Interactions.
525 *Annual Review of Phytopathology*, *45*(1), 437–456.
526 Filhol, O., Nueda, A., Martel, V., Gerber-Scokaert, D., Benitez, M. J., Souchier, C., … Cochet, C.
527 (2003). Live-Cell Fluorescence Imaging Reveals the Dynamics of Protein Kinase CK2
528 Individual Subunits. *Molecular and Cellular Biology*, *23*(3), 975–987.
529 https://doi.org/10.1128/MCB.23.3.975-987.2003
530 Frege, T., & Uversky, V. N. (2015). Intrinsically disordered proteins in the nucleus of human cells.
531 *Biochemistry and Biophysics Reports*, *1*, 33–51. https://doi.org/10.1016/j.bbrep.2015.03.003
532 Glover, C. V. (1986). A Filamentous Form of Drosophila Casein Kinase II. *The Journal of*
533 *Biological Chemistry*, *261*(30), 14349–14354.
534 Götz, C., & Montenarh, M. (2016). Protein kinase CK2 in development and differentiation
535 (Review). *Biomedical Reports*. https://doi.org/10.3892/br.2016.829
536 Han, P., Jin, F. J., Maruyama, J., & Kitamoto, K. (2014). A Large Nonconserved Region of the
537 Tethering Protein Leashin Is Involved in Regulating the Position, Movement, and Function
538 of Woronin Bodies in Aspergillus oryzae. *Eukaryotic Cell*, *13*(7), 866–877.
539 https://doi.org/10.1128/EC.00060-14
540 Hübner, G. M., Larsen, J. N., Guerra, B., Niefind, K., Vrecl, M., & Issinger, O.-G. (2014). Evidence
541 for aggregation of protein kinase CK2 in the cell: a novel strategy for studying CK2
542 holoenzyme interaction by BRET2. *Molecular and Cellular Biochemistry*, *397*(1–2), 285–
543 293. https://doi.org/10.1007/s11010-014-2196-y

544 Josefsen, L., Droce, A., Sondergaard, T. E., Sørensen, J. L., Bormann, J., Schäfer, W., … Olsson, S.
545 (2012). Autophagy provides nutrients for nonassimilating fungal structures and is necessary
546 for plant colonization but not for infection in the necrotrophic plant pathogen Fusarium
547 graminearum, *8*(3), 13.
548 Kershaw, M. J., & Talbot, N. J. (2009). Genome-wide functional analysis reveals that infection-
549 associated fungal autophagy is necessary for rice blast disease. *Proceedings of the National*
550 *Academy of Sciences*, *106*(37), 15967–15972. https://doi.org/10.1073/pnas.0901477106
551 Klionsky, D. J., Abdelmohsen, K., Abe, A., Abedin, M. J., Abeliovich, H., Acevedo Arozena,
552 A., … Zughaier, S. M. (2016). Guidelines for the use and interpretation of assays for
553 monitoring autophagy (3rd edition). *Autophagy*, *12*(1), 1–222.
554 https://doi.org/10.1080/15548627.2015.1100356
555 Kragler, F. (2013). Plasmodesmata: intercellular tunnels facilitating transport of macromolecules in
556 plants. *Cell and Tissue Research*, *352*(1), 49–58. https://doi.org/10.1007/s00441-012-1550-1
557 Lai, J., Koh, C. H., Tjota, M., Pieuchot, L., Raman, V., Chandrababu, K. B., … Jedd, G. (2012).
558 Intrinsically disordered proteins aggregate at fungal cell-to-cell channels and regulate
559 intercellular connectivity. *Proceedings of the National Academy of Sciences*, *109*(39),
560 15781–15786. https://doi.org/10.1073/pnas.1207467109
561 Litchfield, D. W. (2003). Protein kinase CK2: structure, regulation and role in cellular decisions of
562 life and death. *Biochemical Journal*, *369*(1), 1–15.
563 Liu, W., Xie, S., Zhao, X., Chen, X., Zheng, W., Lu, G., … Wang, Z. (2010). A homeobox gene is
564 essential for conidiogenesis of the rice blast fungus Magnaporthe oryzae. *Molecular Plant-*
565 *Microbe Interactions*, *23*(4), 366–375.

566 Liu, X., & Lin, F. (2008). Investigation of the biological roles of autophagy in appressorium
567 morphogenesis in Magnaporthe oryzae. *Journal of Zhejiang University SCIENCE B*, *9*(10),
568 793–796. https://doi.org/10.1631/jzus.B0860013
569 Livak, K. J., & Schmittgen, T. D. (2001). Analysis of Relative Gene Expression Data Using Real-
570 Time Quantitative PCR and the 2−ΔΔCT Method. *Methods*, *25*(4), 402–408.
571 https://doi.org/10.1006/meth.2001.1262
572 Meggio, F., & Pinna, L. A. (2003). One thousand-and one substrates of protein kinase CK2. *The*
573 *FASEB Journal*, *17*, 349–368.
574 Mehra, A., Shi, M., Baker, C. L., Colot, H. V., Loros, J. J., & Dunlap, J. C. (2009). A Role for
575 Casein Kinase 2 in the Mechanism Underlying Circadian Temperature Compensation. *Cell*,
576 *137*(4), 749–760. https://doi.org/10.1016/j.cell.2009.03.019
577 Neijssen, J., Herberts, C., Drijfhout, J. W., Reits, E., Janssen, L., & Neefjes, J. (2005). Cross-
578 presentation by intercellular peptide transfer through gap junctions. *Nature*, *434*, 83–88.
579 Ng, S. K., Liu, F., Lai, J., Low, W., & Jedd, G. (2009). A Tether for Woronin Body Inheritance Is
580 Associated with Evolutionary Variation in Organelle Positioning. *PLoS Genetics*, *5*(6),
581 e1000521. https://doi.org/10.1371/journal.pgen.1000521
582 Padmanabha, R., Chen-Wu, J. L.-P., Arnot, D. E., & Glover, C. V. C. (1990). Isolation, sequencing,
583 and disruption of the yeast CKA2 gene casein kinase II is essential for viability in
584 Saccharomyces cerevisiae. *Molecular And Cellular Biology*, *10*(8), 4089–4099.
585 Plamann, M. (2009). Cytoplasmic Streaming in Neurospora: Disperse the Plug To Increase the
586 Flow? *PLoS Genetics*, *5*(6), e1000526. https://doi.org/10.1371/journal.pgen.1000526
587 Poole, A., Poore, T., Bandhakavi, S., McCann, R. O., Hanna, D. E., & Glover, C. V. (2005). A
588 global view of CK2 function and regulation. *Molecular and Cellular Biochemistry*, *274*(1–
589 2), 163–170.

590 Rao, S., Gerbeth, C., Harbauer, A., Mikropoulou, D., Meisinger, C., & Schmidt, O. (2011).
591 Signaling at the gate: Phosphorylation of the mitochondrial protein import machinery. *Cell*
592 *Cycle*, *10*(13), 2083–2090. https://doi.org/10.4161/cc.10.13.16054
593 Rosenberger, A. F. N., Morrema, T. H. J., Gerritsen, W. H., van Haastert, E. S., Snkhchyan, H.,
594 Hilhorst, R., … Hoozemans, J. J. M. (2016). Increased occurrence of protein kinase CK2 in
595 astrocytes in Alzheimer's disease pathology. *Journal of Neuroinflammation*, *13*(1).
596 https://doi.org/10.1186/s12974-015-0470-x
597 Seetoh, W.-G., Chan, D. S.-H., Matak-Vinković, D., & Abell, C. (2016). Mass Spectrometry
598 Reveals Protein Kinase CK2 High-Order Oligomerization *via* the Circular and Linear
599 Assembly. *ACS Chemical Biology*, *11*(6), 1511–1517.
600 https://doi.org/10.1021/acschembio.6b00064
601 Shen K-F., Osmani A. S., Govindaraghavan M., & Osmani S. A. (2014). Mitotic rregulation of
602 fungal cell-to-cell connectivity through septal pores involves the NIMA kinase. *Molecular*
603 *Biology of the Cell*, *25*, 763–775. https://doi.org/10.1091/mbc.E13-12-0718
604 Shlezinger, N., Goldfinger, N., & Sharon, A. (2012). Apoptotic-like programed cell death in fungi:
605 the benefits in filamentous species. *Frontiers in Oncology*, *2*.
606 https://doi.org/10.3389/fonc.2012.00097
607 Talbot, N. J., Kershaw, M. J., Wakley, G. E., De Vries, O. M., Wessels, J. G., & Hamer, J. E.
608 (1996). MPG1 encodes a fungal hydrophobin involved in surface interactions during
609 infection-related development of Magnaporthe grisea. *The Plant Cell Online*, *8*(6), 985–999.
610 Uversky, V. N. (2015). The multifaceted roles of intrinsic disorder in protein complexes. *FEBS*
611 *Letters*, *589*(19PartA), 2498–2506. https://doi.org/10.1016/j.febslet.2015.06.004
612 Valero, E., De Bonis, S., Filhol, O., Wade, R. H., Langowski, J., Chambaz, E. M., & Cochet, C.
613 (1995). Quaternary Structure of Casein Kinase 2 - Characterization of Multiple Oligomeric

614 States and Relation with its Catalytic Activity. *The Journal of Biological Chemistry*,
615 *270*(14), 8345–8352.
616 Veneault-Fourrey, C. (2006). Autophagic Fungal Cell Death Is Necessary for Infection by the Rice
617 Blast Fungus. *Science*, *312*(5773), 580–583. https://doi.org/10.1126/science.1124550
618 Villalba, F., Collemare, J., Landraud, P., Lambou, K., Brozek, V., Cirer, B., … Lebrun, M.-H.
619 (2008). Improved gene targeting in Magnaporthe grisea by inactivation of MgKU80
620 required for non-homologous end joining. *Fungal Genetics and Biology*, *45*(1), 68–75.
621 https://doi.org/10.1016/j.fgb.2007.06.006
622 Vucetic, S., Brown, C. J., Dunker, A. K., & Obradovic, Z. (2003). Flavors of protein disorder.
623 *Proteins: Structure, Function, and Bioinformatics*, *52*(4), 573–584.
624 Wang, C., Zhang, S., Hou, R., Zhao, Z., Zheng, Q., Xu, Q., … Xu, J.-R. (2011). Functional
625 Analysis of the Kinome of the Wheat Scab Fungus Fusarium graminearum. *PLoS Pathogens*,
626 *7*(12), e1002460. https://doi.org/10.1371/journal.ppat.1002460
627 Wang, X., & Johnsson, N. (2005). Protein kinase CK2 phosphorylates Sec63p to stimulate the
628 assembly of the endoplasmic reticulum protein translocation apparatus. *Journal of Cell*
629 *Science*, *118*(4), 723–732. https://doi.org/10.1242/jcs.01671
630 Wong, E., & Cuervo, A. M. (2010). Integration of Clearance Mechanisms: The Proteasome and
631 Autophagy. *Cold Spring Harbor Perspectives in Biology*, *2*(12), a006734–a006734.
632 https://doi.org/10.1101/cshperspect.a006734
633 Wright, P. E., & Dyson, H. J. (2015). Intrinsically disordered proteins in cellular signalling and
634 regulation. *Nature Reviews Molecular Cell Biology*, *16*(1), 18–29.
635 https://doi.org/10.1038/nrm3920

636 Zare-shahabadi, A., Masliah, E., Johnson, G. V. W., & Rezaei, N. (2015). Autophagy in
637 Alzheimer's disease. *Reviews in the Neurosciences*, *26*(4). https://doi.org/10.1515/revneuro-
638 2014-0076
639 Zetina, C. R. (2001). A Conserved Helix-Unfolding Motif in the Naturally Unfolded Proteins.
640 *Proteins: Structure, Functions, and Genetics*, *44*, 479–483.

641

642 **Acknowledgements** We thank Dr. Guanghui Wang, Dr. Wenhui Zheng, Dr. Ya Li and
643 Dr. Huawei Zheng (Fujian Agriculture and Forestry University, Fuzhou, China) for
644 their helpful discussions. We thank Professor Jin-Rong Xu, Department of Botany
645 and Plant Pathology Purdue University, U.S.A. for providing the Ku80 strain. We
646 thank Dr. Bjoern Oest Hansen, Goettingen for help with mapping and constructing
647 the used *M. oryzae* transcriptome datafile from downloaded data. This work was
648 supported by the National Natural Science Foundation of China (U1305211),
649 National Key Research and Development Program of China (2016YFD0300700) and
650 National Natural Science Foundation for Young Scientists of China (Grant
651 No.31500118 and No.31301630).

652 **Authors' contributions** Conceived and designed the experiments: G. L., S. O. and Z.
653 W. Performed the experiments: L. Z., D. Z., Y. C., W. Y. and Q. L. Analysed the data:
654 L. Z., D. Z., S. O. and Z. W. Wrote the paper: L. Z., D. Z., S. O. and Z. W.

655 **Competing interests statement** The authors declare that they have no competing
656 financial interests.

657 **Correspondence** and request for materials should be addressed to S.O.
658 (stefan@olssonstefan.com) or Z.W. (wangzh@fafu.edu.cn).

659

660

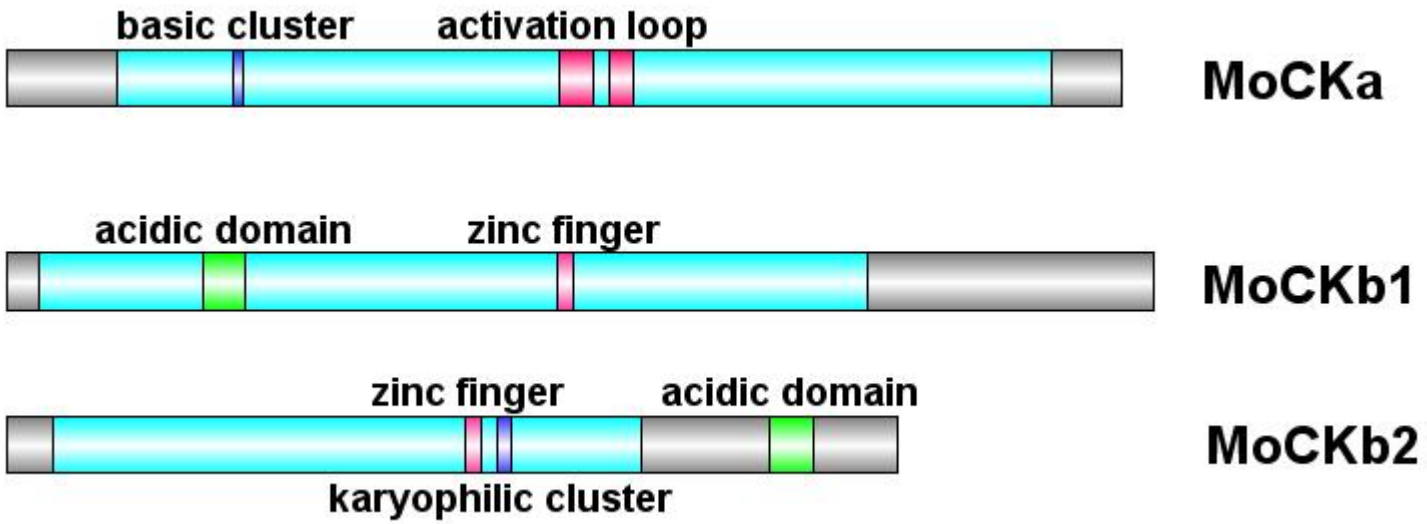

Figure 1. Domain structure of the identified CK2 proteins.
MoCKa sequence (341 aa) was obtained from NCBI and the 35-320 region contains the protein kinase domain (https://www.ncbi.nlm.nih.gov/nuccore/XM_003716137.1) is labelled light blue, 70-73 is the basic cluster labelled dark blue and functions as a nuclear localization signal (NLS), 170-180 and 185-192 are activation loops (A-loop) labelled red.
MoCKb1 sequence (351 aa) was obtained from NCBI and the 11-264 region contains the Casein kinase II regulatory domain (https://www.ncbi.nlm.nih.gov/protein/XP_003718622.1) labelled light blue, 61-74 is the acidic domain labelled green, 169-174 is the zinc finger domain labelled pink.
MoCKb2 sequence (273 aa) was obtained from NCBI and the 15-195 region is the Casein kinase II regulatory subunit domain (https://www.ncbi.nlm.nih.gov/protein/XP_003710544.1) labelled light blue, 141-146 is a zinc finger labelled pink, 151-155 is a karyophilic cluster labelled dark blue that functions as a NLS, 234-247 is an acidic domain labelled green. The illustration was made using the DOG 2.0 Visualization of Protein Domain Structures http://dog.biocuckoo.org/.

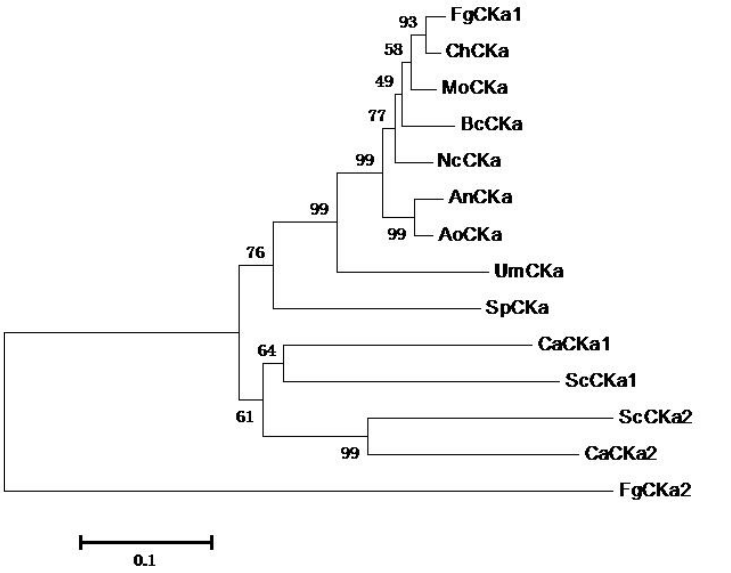

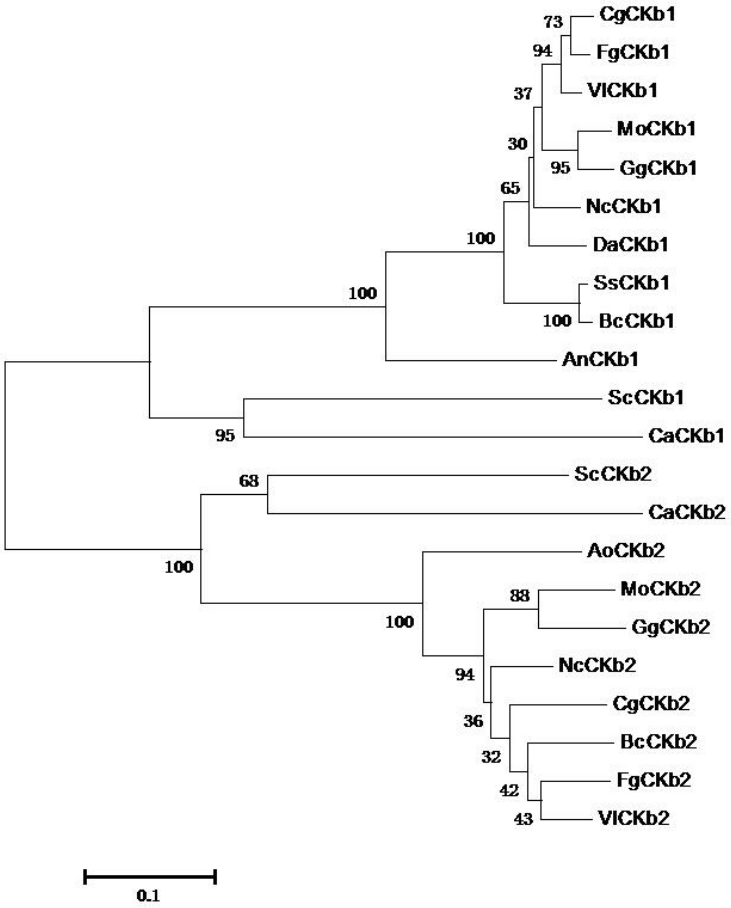

Figure 1 Supplement 1 (**a**) Phylogenetic analysis of CKa amino acid sequences from a range of organisms. A neighbor-joining tree was constructed from amino acid sequences of a range of CKa-encoding genes from diverse fungi. Tree topology was tested by 1000 bootstrap resampling of the data. Full species names and access codes for the annotated genes are given in Figure 1 Supplement 2 legend. **(b)** Phylogenetic analysis of CKb amino acid sequences from a range of organisms. A neighbor-joining tree was constructed from amino acid sequences of a range of CKb-encoding genes from diverse fungi. Tree topology was tested by 1000 bootstrap resampling of the data. Full species names and access codes for the annotated genes are given in Figure 1 Supplement 3 and Figure 1 Supplement 4 legends.

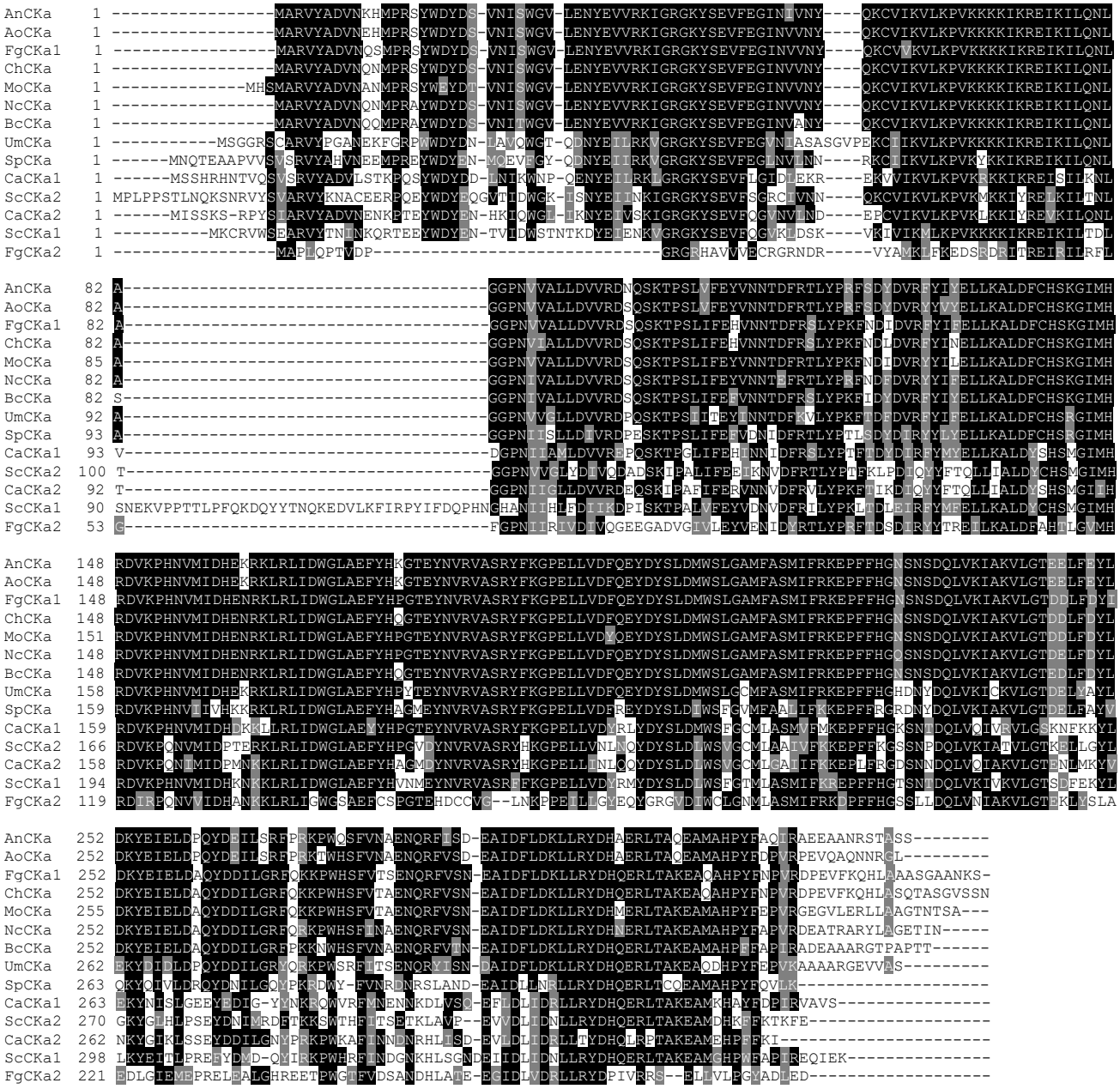

Figure 1 Supplement 2. Alignment of predicted amino acid sequences of CKa from different fungi. Sequence for the CKa in *M. oryzae* and other fungi were aligned using ClustalW and shaded by Boxshade 3.2. Identical amino acids are highlighted on a black background and similar amino acids on a light grey background. The *M. oryzae* amino acid sequence is aligned with the sequences of the putative homologs:

AnCKa (*Aspergillus nidulans*, EAA64615.1),
AoCKa (*Aspergillus oryzae*, KDE76853.1),
FgCKa1 (*Fusarium graminearum*, EYB33507.1),
FgCKa2 (*F. graminearum*, EYB32538.1),
ChCKa (*Colletotrichum higginsianum*, CCF36406.1),
MoCKa (*M. oryzae,* EHA49866.1),
NcCKa (*N. crassa*, EAA35747.3),
BcCKa (*Botrytis cinerea*, EMR85876.1),
UmCKa (*Ustilago maydis*, XP_011387122.1),
SSpCKa (*Schizosaccharomyces pombe*, CAA52331.1),
CaCKa1 (*Candida albicans*, KGU14189.1),
CaCKa2 (*C. albicans*, KGU00855.1),
ScCKa1 (*S. cerevisiae*, EDN61459.1),
ScCKa2 (*S. cerevisiae*, EDN63928.1).

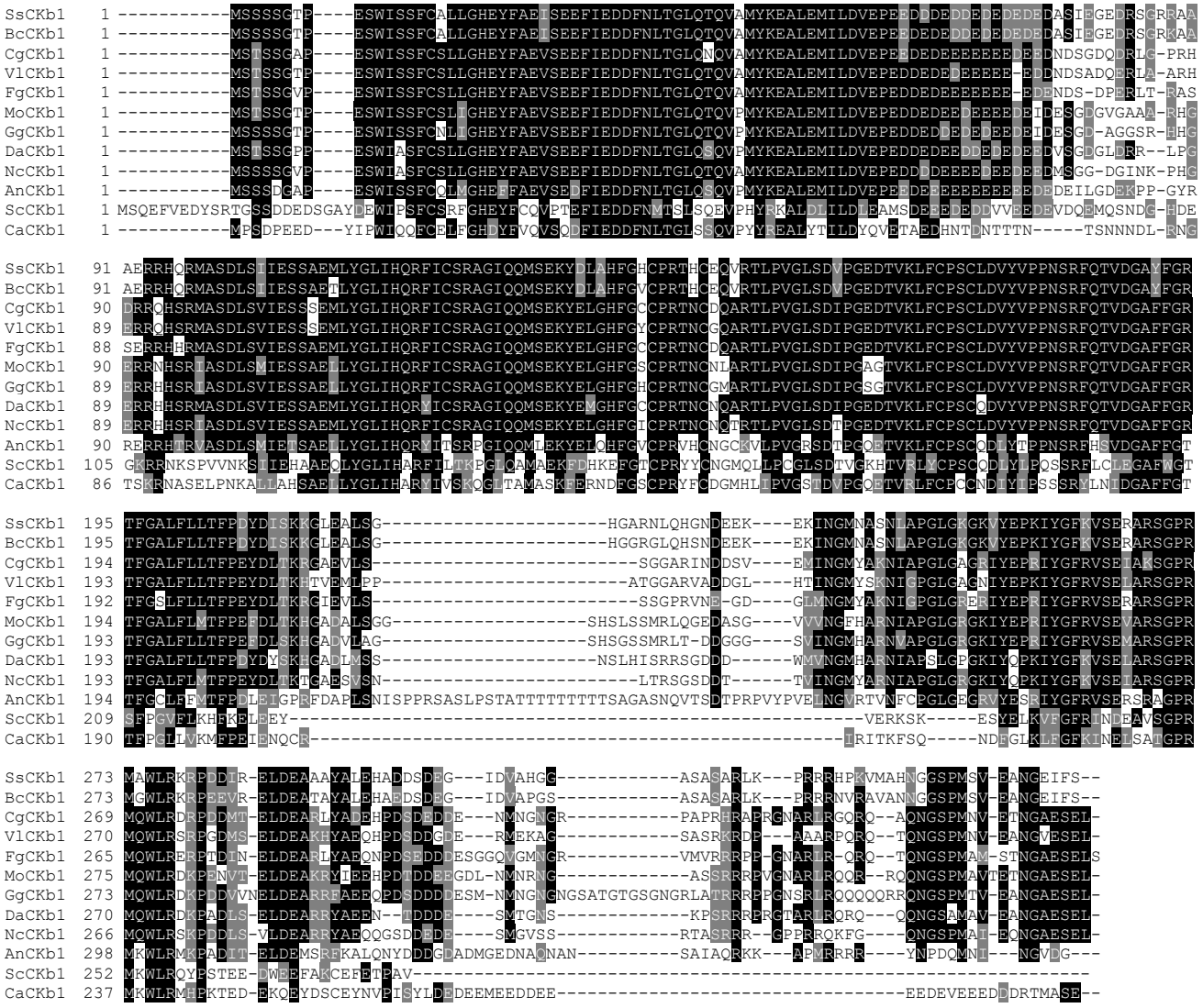

Figure 1 Supplement 3. Alignment of predicted amino acid sequences of CKb1 from different fungi. Sequence for the CKb1 in *M. oryzae* and other fungi were aligned using ClustalW and shaded by Boxshade 3.2. Identical amino acids are highlighted on a black background and similar amino acids on a light grey background. The *M. oryzae* amino acid sequence is aligned with the sequences of the putative homologs:

MoCKb1 (*M. oryzae*, XP_003718622.1),
GgCKb1 (*Gaeumannomyces graminis*, XP_009229023.1)
CgCKb1 (*Colletotrichum graminicola*, XP_008099475.1),
NcCKb1 (*N. crassa*, XP_960447.1),
FgCKb1 (*F. graminearum*, XP_011320142.1),
SsCKb1 (*Sclerotinia sclerotiorum*, XP_001592667.1),
BcCKb1 (*B. cinerea*, XP_001546938.1),
DaCKb1 (*Diaporthe ampelina*, KKY35702.1),
VlCKb1 (*Verticillium longisporum*, CRK29524.1),
AnCKb1 (*A. nidulans*, CBF77758.1),
ScCKb1 (*S. cerevisiae,* NP_011496.3),
CaCKb1 (*C. albicans*, KHC46950.1).

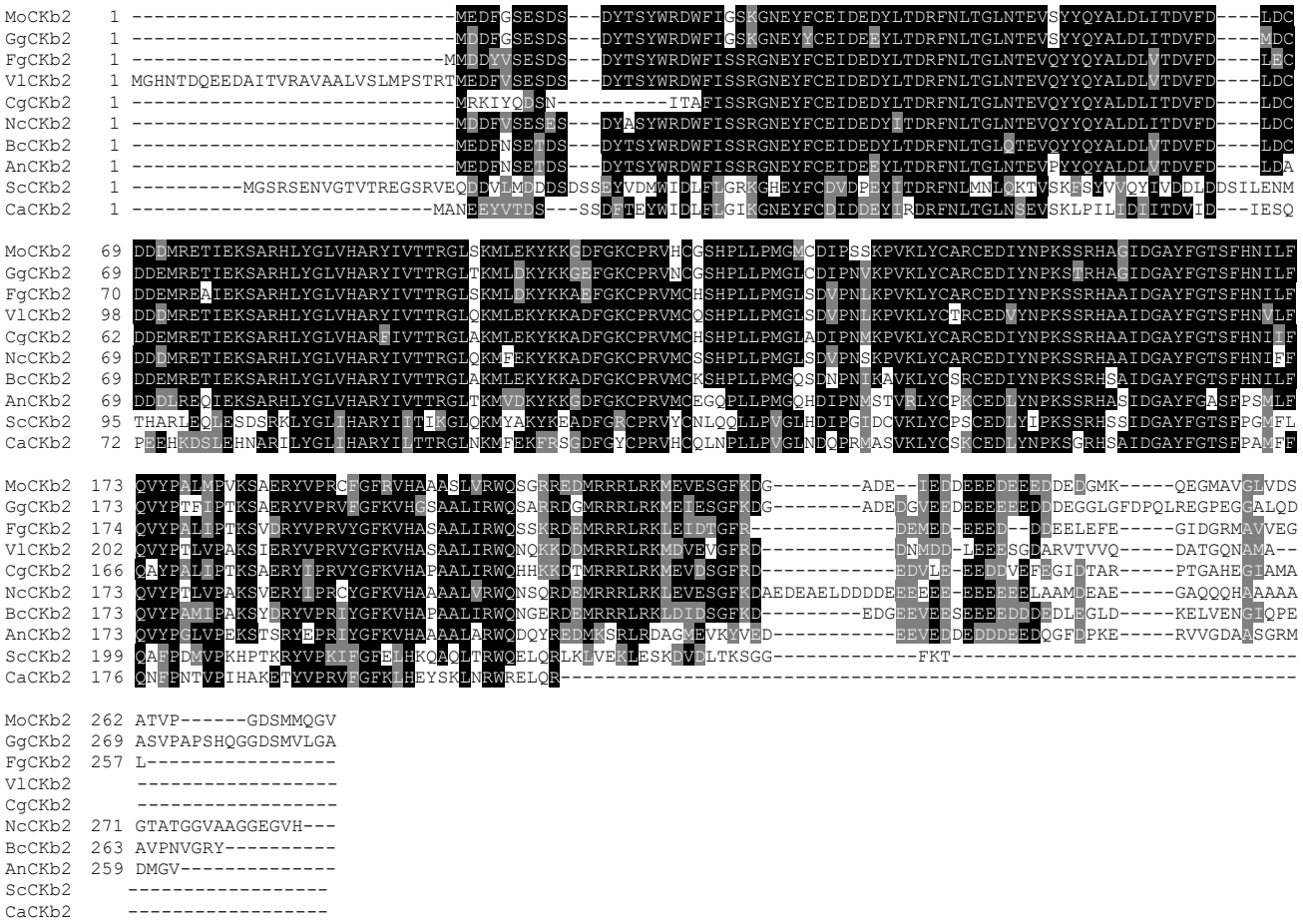

Figure 1 Supplement 4. Alignment of predicted amino acid sequences of CKb2 from different fungi. Sequence for the CKb2 in *M. oryzae* and other fungi were aligned using ClustalW and shaded by Boxshade 3.2. Identical amino acids are highlighted on a black background and similar amino acids on a light grey background. The *M. oryzae* amino acid sequence is aligned with the sequences of the putative homologs:

MoCKb2 (*M. oryzae*, XP_003710544.1),
GgCKb2 (*G. graminis*, XP_009217338.1),
FgCKb2 (*F. graminearum*, EYB21652.1),
VlCKb2 (*V. longisporum*, CRK18911.1),
CgCKb2 (*C. graminicola*, XP_008092732.1),
NcCKb2 (*N. crassa*, XP_001728406.1),
BcCKb2 (*B. cinerea*, XP_001558441.1),
AnCKb2 (*A. nidulans*, XP_001825358.2),
ScCKb2 (*S. cerevisiae*, AAT93000.1),
CaCKb2 (*C. albicans*, EEQ46313.1).

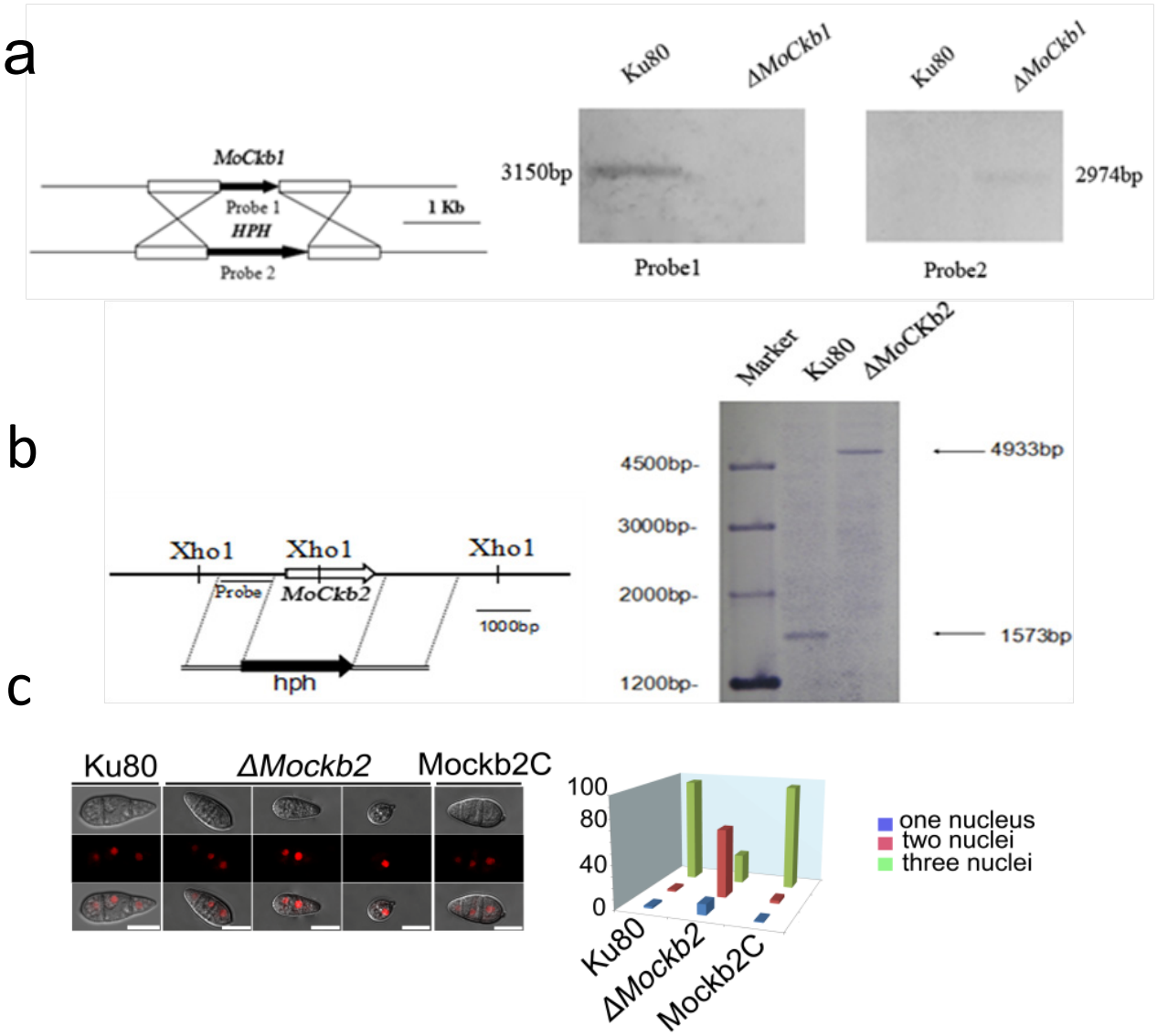

Figure 2. Knockout of the MoCKbs and the effect of this on conidia morphology and MoCKa gene expression (**a**) *ΔMoCkb1* mutant was verified by Southern blot analysis. The genomic DNA extracted from the strains Ku80 and the mutant *ΔMoCkb1* was digested with *Nde1* and tested by Southern blot. The different probes ORF and hph were amplified from the genomic DNA of the wild type Ku80 and the plasmid pCX62 respectively.
(**b**) *ΔMoCkb2* mutant was verified by Southern blot analysis. The genomic DNA extracted from the strains *Ku80* and the mutant *ΔMoCkb2* was digested with *Xho1* and tested by Southern blot. The probe was amplified from the genomic DNA of the background strain Ku80.
(**c**) The conidial morphology of the *ΔMockb2* deletion was detected. The red fluorescence show the nuclear number in the conidia. The red fluorescence was due to the nuclear protein histone linker (MGG_12797) fused with mCherry used as nuclear marker. All bars = 10 um. The percentage of conidia with different nuclear number in the conidia produced by the background strain Ku80, the *ΔMockb2* deletion mutant and in the complementation strain MoCKb2C.

Figure 3. Control that GFP-MoCKa, GFP-MoCKb1 and GFP-MoCKb2 are as pathogenic as the background Ku80. CK is untreated control.

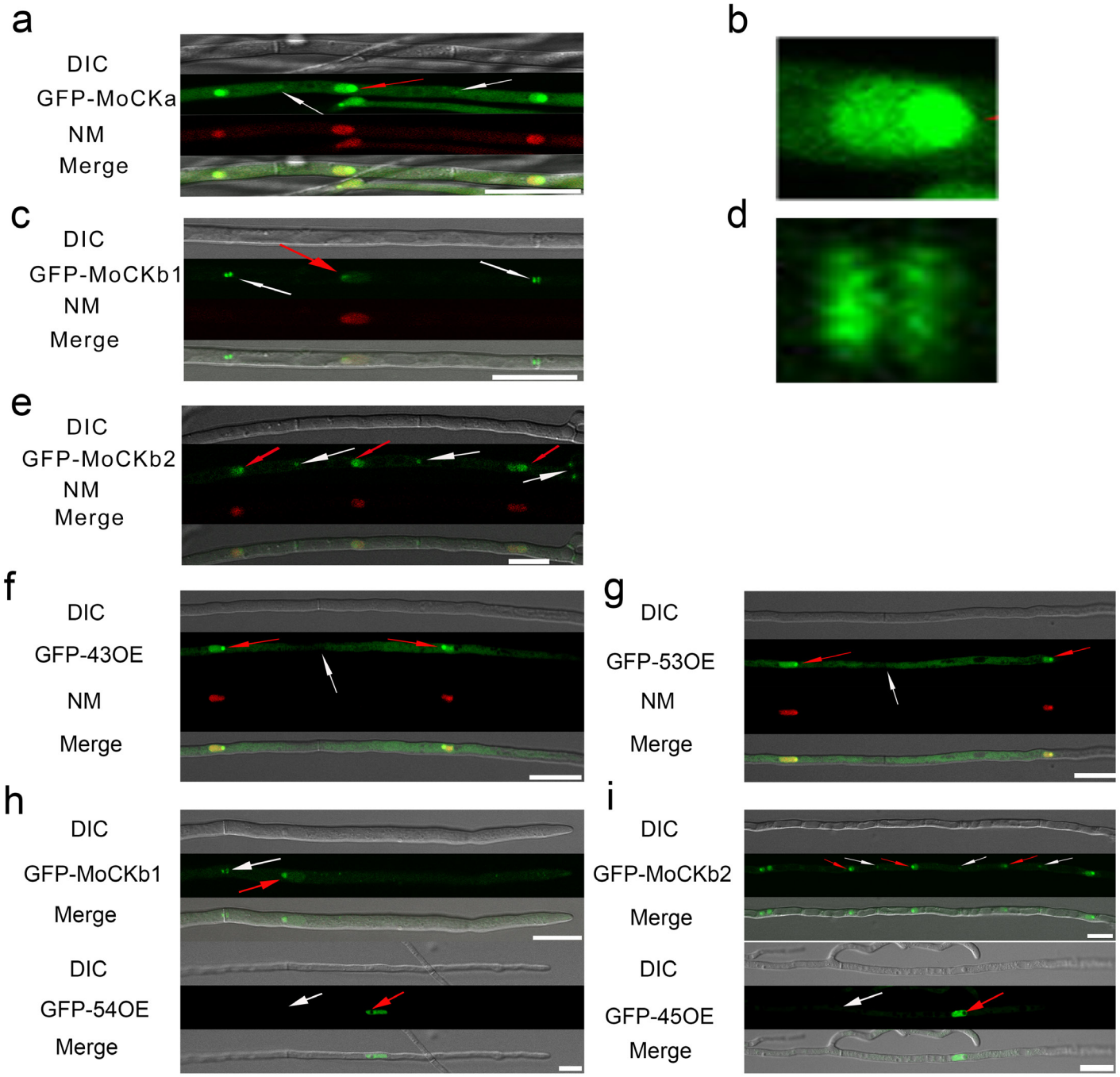

Figure 4. Intracellular localization of the three CK2 holoenzyme components showing that all three proteins are needed for normal localization. a-e, Localization of the three MoCK2 subunits in the background strain Ku80. The background strain Ku80 was transformed through gene replacements using plasmids containing GFP-MoCKa, GFP-MoCKb1 and GFP-MoCKb2. All three GFP constructs localize preferentially to nucleoli and to septal pores between cells. **b**, Enlargement of the nuclear localization of GFP-MoCKa (marked with red arrow in **a**). **d**, Enlargement of the septal localization of GFP-MoCKb1 (left septa marked with white arrow in **c**) **f** and **g**, Localization of over expressed GFP-MoCKa in *ΔMockb1* (43OE-GFP) or in *ΔMockb2* (53OE-GFP) does not rescue normal localization to septal pores. **h** and **i**, (below) Neither overexpression of MoCKb1 in *ΔMockb2* (54OE-GFP) nor overexpression of MoCKb2 in *ΔMockb1* (45OE-GFP) rescued normal localization (GFP-MoCKb1 and GFP-MoCKb2) (above) to nucleoli or septal pores. Histone linker (MGG_12797) was fused with the mCherry and used as nuclear localization marker (NM). All bars=10mm.

Figure 4 Supplement 1.
GFP-MoCKa localization in conidia.

Magnaporthe oryzae conidia.

GFP-MoCKa localizes to nuclei (red arrows) and to septal pores (white arrows). White bar is 10 μm.

a

Expression of	Control	Test	Test/control	SE (N=9)	P=same or higher than control
MoCKa	Ku80	*ΔMoCKb1*	0.38	0.01	2.07E-11
MoCKa	Ku80	*ΔMoCKb2*	0.54	0.05	5.12E-06

b

Expression of	Control	Test	Test/control	SE (N=9)	P=same or lower than control
MoCKa	ΔMoCKb1	43OE	25.11	1.32	4.23E-08
MoCKa	ΔMoCKb2	53OE	14.60	1.45	6.85E-06

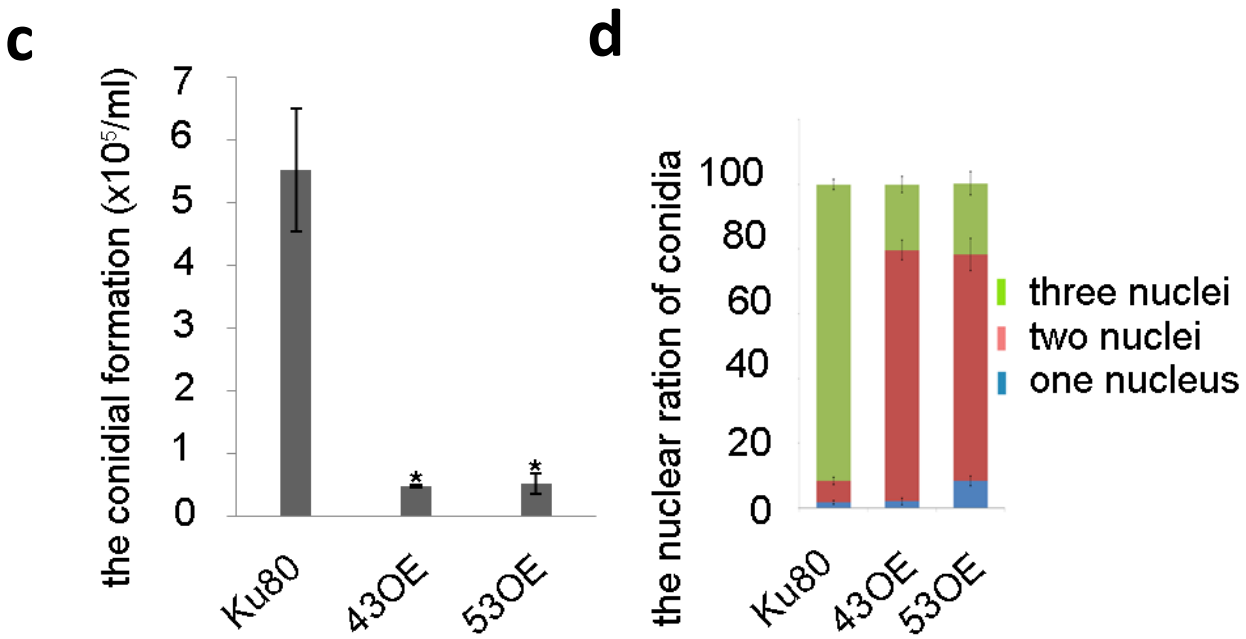

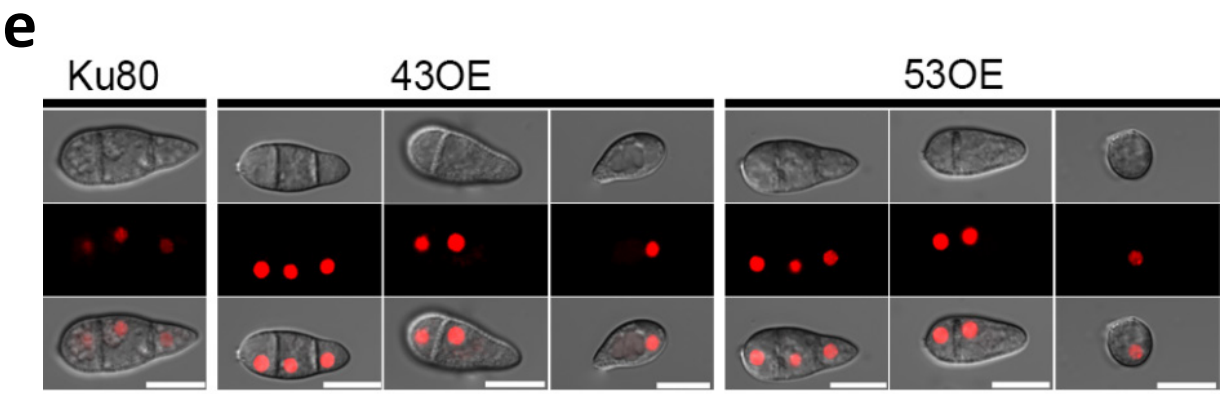

Figure 5. Overexpression of MoCKa in the MoCKb deletion mutants and the effect of this on conidia morphology. (**a**) MoCKa expression in the *ΔMockb1* and *ΔMockb2* deletion relative to the MoCKa expression in the control Ku80 showing that expression of the two CKb were both reduced in the deletion mutants (**b**) The relative expression of MoCKa in the 43OE and 53OE in relation to their respective control backgrounds *ΔMoCKb1* and *ΔMoCKb2*. (**c**) The conidial forming ability of the 43OE and 53OE transformants compared to the background strain Ku80. (**d**) The percentage of conidia with different numbers of nuclei produced by the background strain Ku80 and the 43OE and 53OE strains. (**e**) The conidia morphology of 43OE and 53OE transformants. The red fluorescence was due to the nuclear protein histone linker (MGG_12797) fused with the mCherry. All bars = 10 um.

Figure 5 Supplement 1. The expression the different overexpressed components of the MoCK2 holoenzyme in the Ku80 background and the deletion mutant background in relation to the expression in respective background. The experiments were repeated three times with triple replications.

Expression of	Control	Test	Test/control	SE (N=9)	P=same or lower than control
MoCKa	Ku80	GFP-MoCKa	15.38	0.87	8.80E-08
MoCKb1	Ku80	GFP-MoCKb1	9.51	0.70	1.01E-06
MoCKb2	Ku80	GFP-MoCKb2	14.64	0.85	1.14E-07
MoCKb2	*ΔMoCKb1*	45OE	12.63	1.35	1.26E-05
MoCKb1	*ΔMoCKb2*	54OE	45.47	2.52	5.43E-08

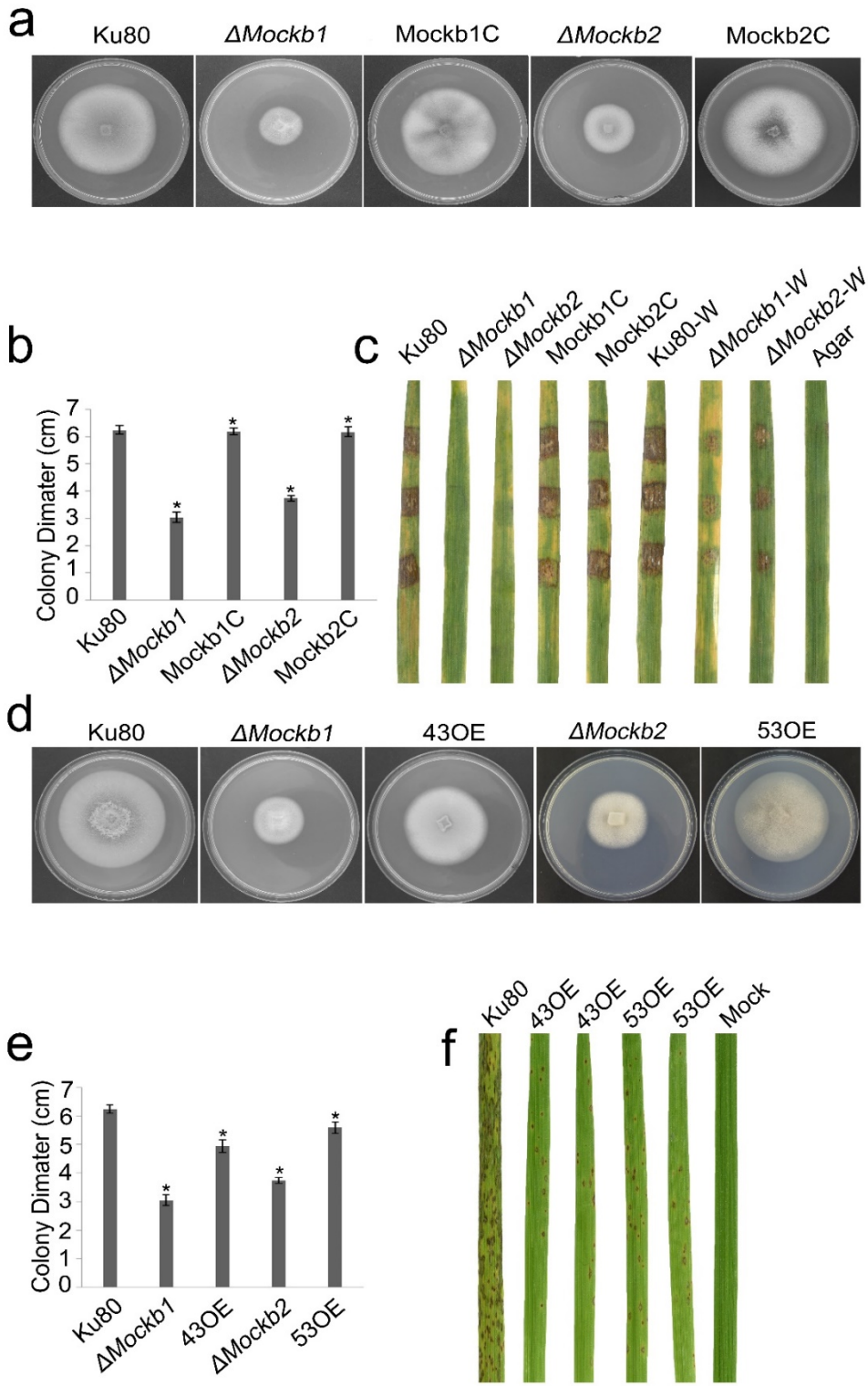

Figure 6. Intact CK2 holoenzyme is needed for normal growth, infection, pathogenicity. a, Colonial morphology and **b,** vegetative growth of *ΔMockb1* and *ΔMockb2* deletion mutants and their respective complementation strains was observed on SYM agar plates incubated in the dark for 10 days at 25°C, and then photographed. **c,** Pathogenicity analysis of *ΔMockb1* and *ΔMockb2* on rice. Disease symptoms on rice leaves of 2-week-old seedlings inoculated using mycelial plugs since mutants produced no or very few conidia. Typical leaves were photographed 6 days after inoculation. The Mockb1C and Mockb2C were complementary strains. Treatments ending with a W indicate that the leaf surface was wounded before the plug was applied. The rice cultivar was CO-39. **d,** Colonial morphology and **e,** vegetative growth of *ΔMockb1*, *ΔMockb2*, and overexpressed CKa-GFP in the *ΔMockb1* (43OE) and in *ΔMockb2* (53OE) transformants were observed on SYM medium agar plates incubated in the dark for 10 days at 25°C, and then photographed. **f,** Pathogenicity analysis of overexpressed CKa-GFP in the *ΔMockb1* (43OE) and in *ΔMockb2* (53OE). Disease symptoms on rice leaves of 2-week-old seedlings inoculated with conidia suspension since CKa overexpressed strains produced just enough conidia to use for the assay. The concentration of conidia in the suspension was about 1×10^5/ml. Typical leaves were photographed 6 days after inoculation. The rice cultivar was CO-39. Error bars shows SE and a star indicate a $P<0.05$ for control is same or larger than for the mutants.

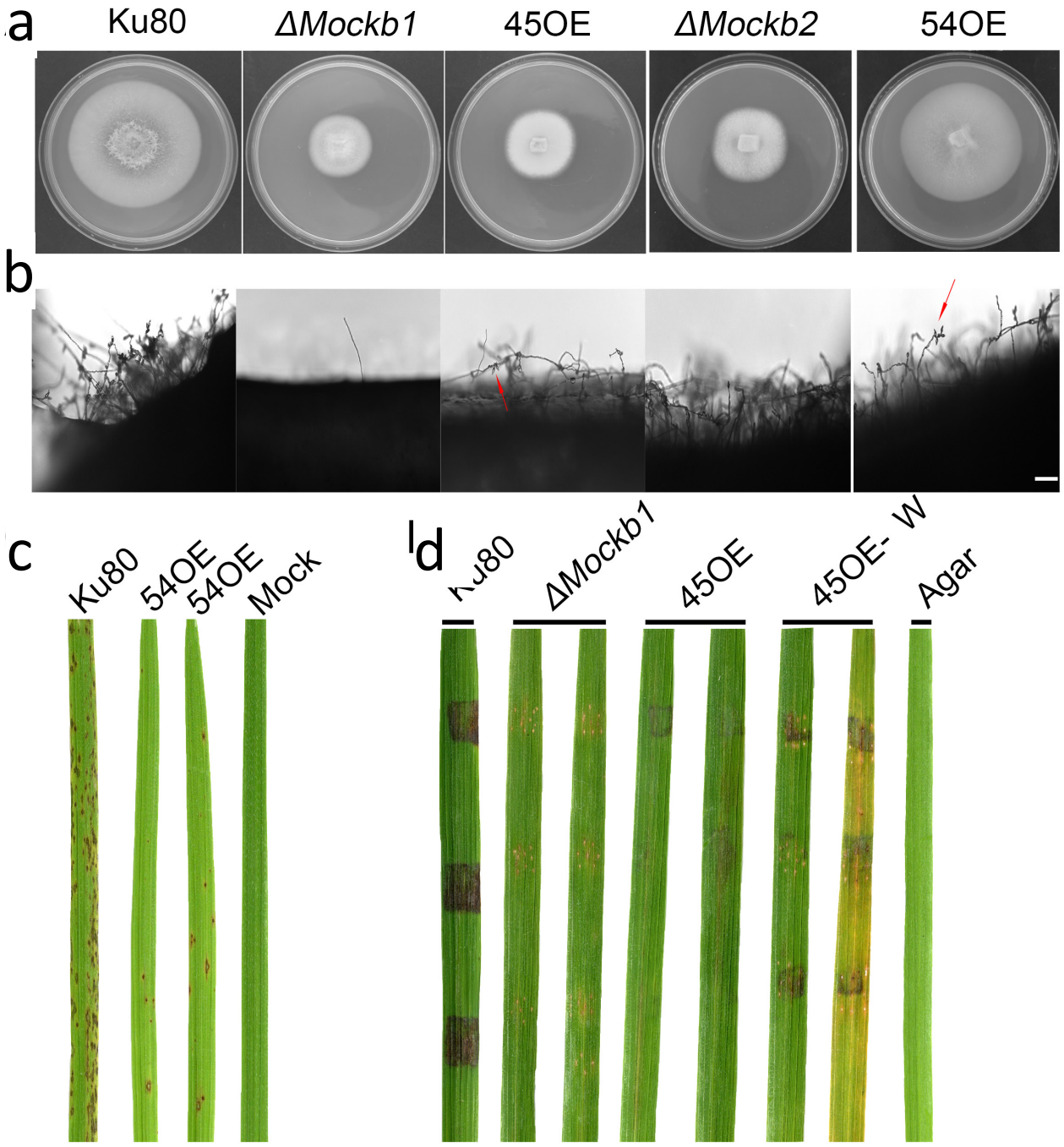

Figure 6 Supplement 1. Phenotypic effects in the respective MoCKb deletion mutants of overexpression the other MoCKb component. (**a** and **c**) Colonial morphology and vegetative growth of *ΔMockb1*, 45OE transformants, *ΔMockb2* and 54OE transformants was observed on SYM medium agar plates grown in the dark for 10 days at 25 °C and then photographed.
(**b**) Development of conidia on conidiophores. Light microscopic observation was performed on strains grown on the rice bran medium for 10 days. The red arrows indicate some conidia are produced by the 45OE and 54OE transformants. Bar=50um.
(**c**) Pathogenic analysis of 54OE transformants on rice was shown above. Disease symptoms on rice leaves of 2-week-old seedlings were also inoculated by conidia suspension. The concentration of conidia suspension for inoculation was about $1x10^5$/ml.
(**d**) Pathogenic analysis of *ΔMockb1* and 45OE transformants on rice. Disease symptoms on rice leaves of 3-week-old seedlings were also inoculated using mycelial plugs. The 45OE-W indicates that the rice leaves were wounded. Typical leaves were photographed 6 days after inoculation. The rice strain was CO-39.

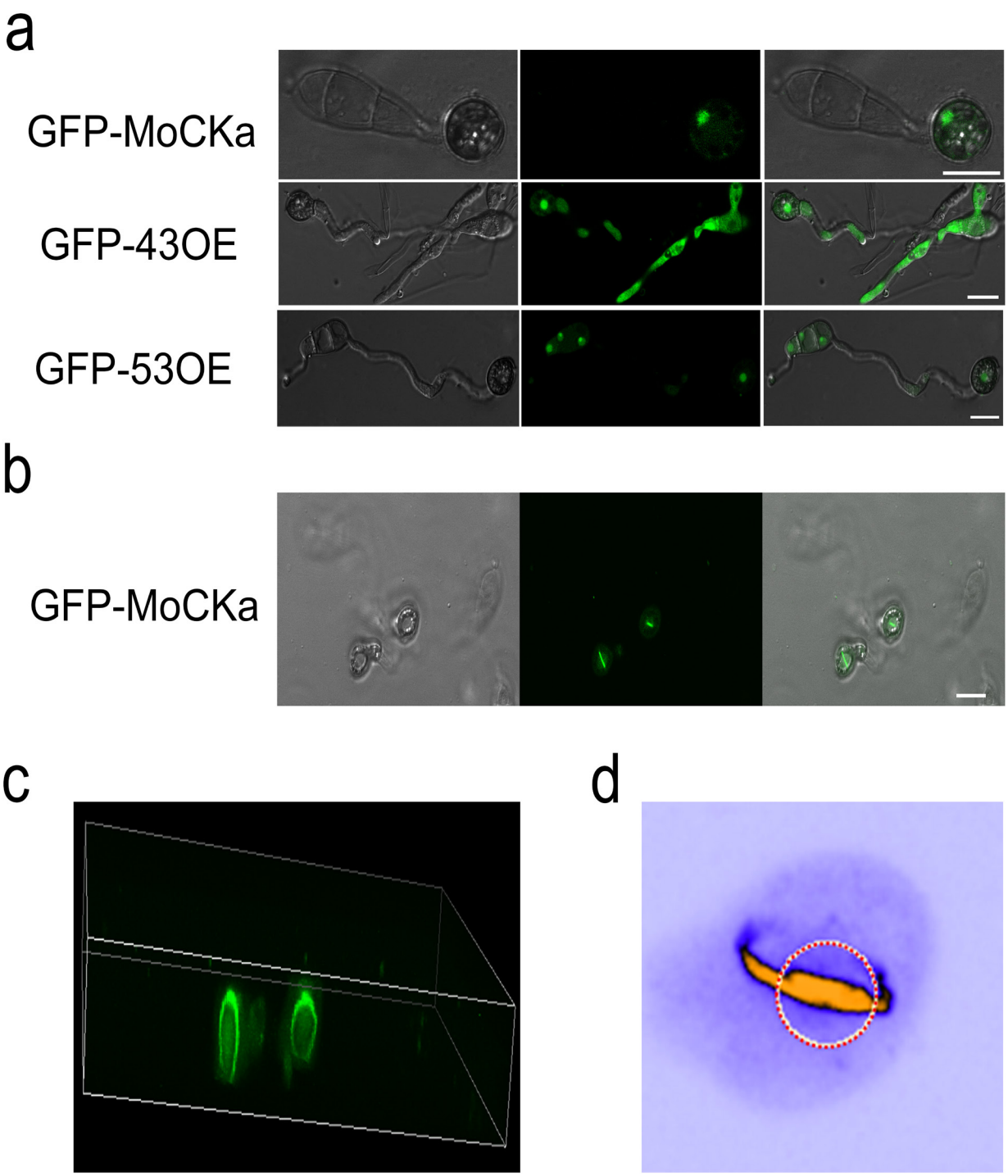

Figure 7. Localization of the GFP-MoCKa subunit in appressoria of the background strain Ku80 the and in the two MoCKb deletion strains (43OE-GFP and 53OE-GFP) (compare Fig. 1a, f, g). **a,** Localization of GFP-MoCKa in all three strains show localization to nuclei**. b,** In the background strain Ku80 that form appressoria from conidia a bright line of GFP-MoCKa can be seen across the appressorium penetration pores. **c.** Through 3d scanning and then rotating the 3d reconstruction image (Link to Movie 1) we found that the streak across the penetration pores is a ring of GFP-MoCKa perpendicular to the penetration pore opening not present in the deletion strains (Link to Movie 2 and 3). **d,** False colour lookup table 3d reconstruction image of the right ring structure in **c** enlarged and rotated back and seen from the same angle as in **b** with the penetration pore opening indicated by a red-white circle seen from the "plant" side (Link to Movie 4 and 5 for left and right ring in false colours). The false colour was used so that the week fluorescence in the cytoplasm could be used to show the whole cytoplasm volume. The image was made using the analytical image analysis freeware ImageJ (https://imagej.nih.gov/ij/index.html) and the ICA lookup table in ImageJ was used for false colouring. **e**, Measurements of the sizes of the GFP-MoCKa rings in seen in **c.** All bars=10 mm.

Figure 7 Supplement 1.
GFP-MoCKa localization in appressoria.

Magnaporthe oryzae appressoria. Image in the 3d stack (left appressorium in Fig. 3b,d) that shows the septal pore accumulation. Image deliberately ”overexposed” to be able to show nuclear and septal localization.

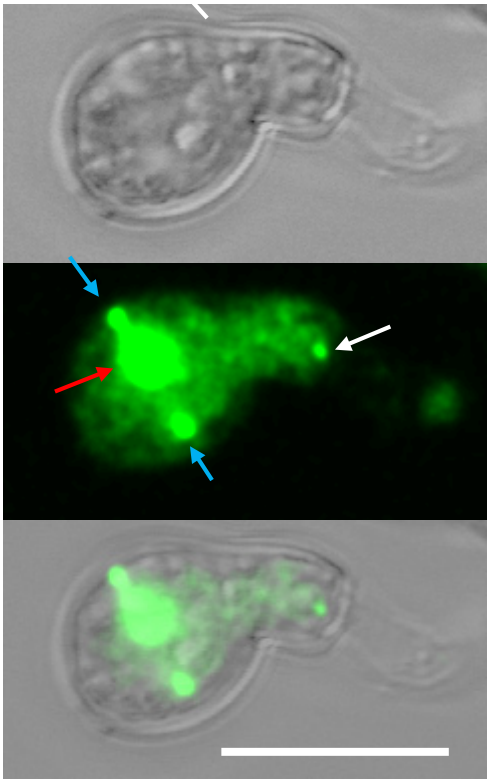

GFP-MoCKa localizes to nuclei (red arrow) surrounded by the MoCK-HRS in cross-section (blue arrows) and to the septal pore towards the germtube (white arrow). White bar is 10 μm.

Figure 7 Supplement 2.

MoCK2 Rings	Right	Left
Measurements from images	um	um
Outer diameter	5.3	5.5
Max thickness at penetration pore	1.4	1.2
Thickness on sides and away from pore	0.7	0.7
Thickness seen from side	0.7	0.7

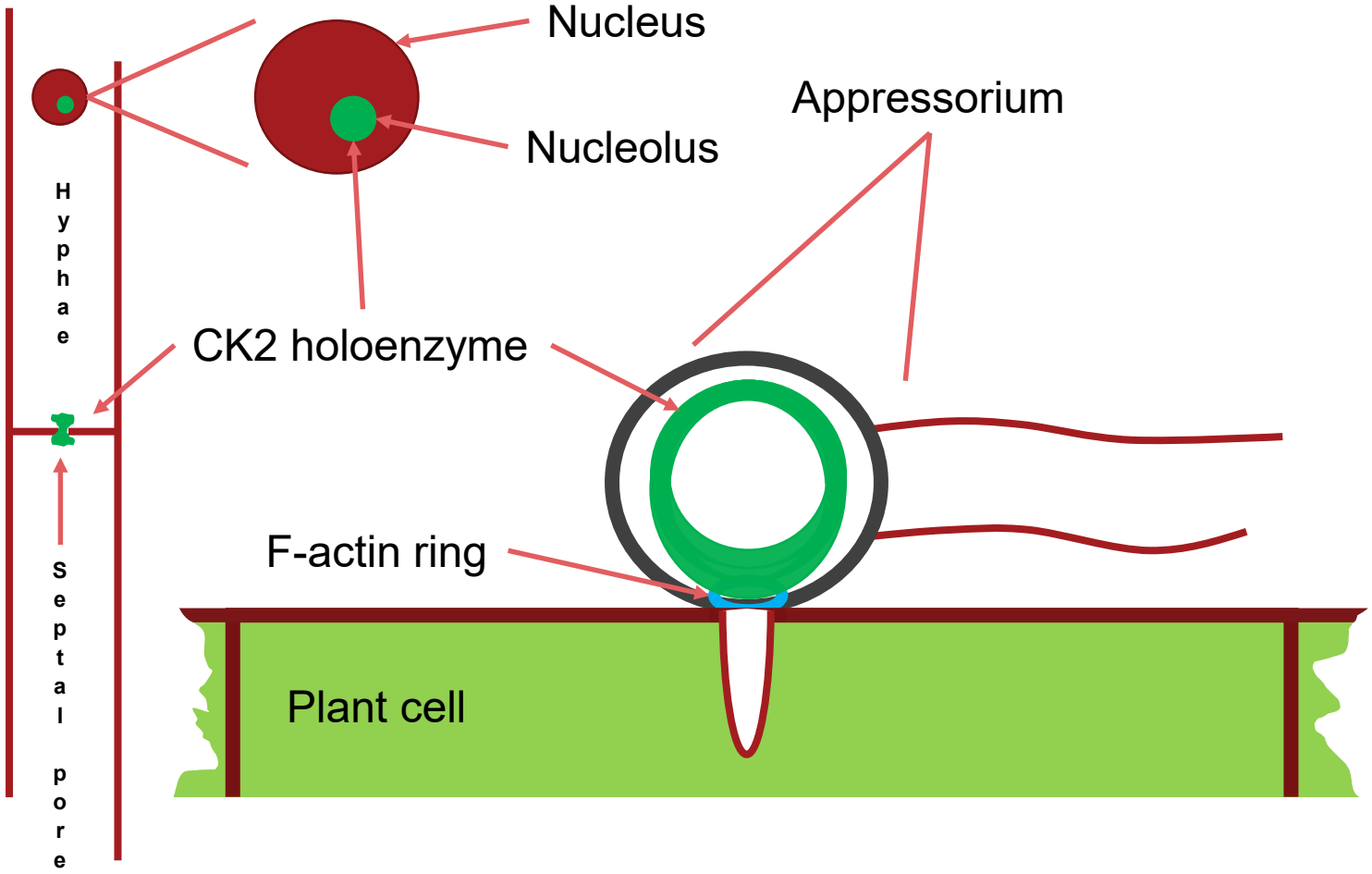

Figure 8. Schematic drawing of the main localizations of the CK2 holoenzyme. It localizes to the nucleolus, to septal pores between cells and forms a CK2-Holoenzyme Ring Structure (CK2-HRS) perpendicular to the F-actin ring surrounding the appressorium penetration pore. Appressorium and hyphae drawn approximately to their relative sizes.

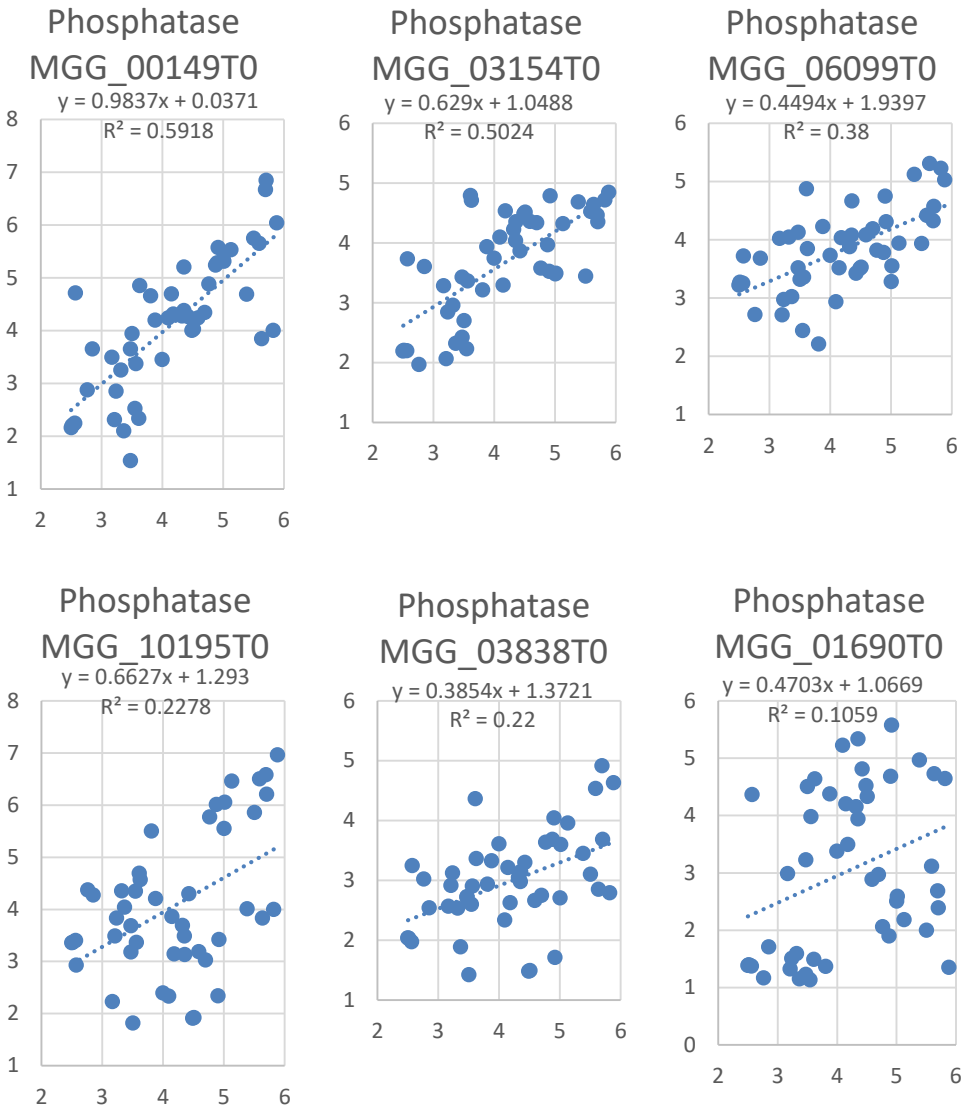

Figure 9. Plots of 6 putative serine/threonine protein phosphatase expression (y-axis) vs MoCKa expression (x-axis) in a range of transcriptome datasets from different experiments (Note: Log2 scale on axes and grids are represented with fixed "aspect ratio" to highlight the different slopes of the correlations). MGG_01690 is not in the pulldown while the other five are and used to illustrate that all S/T phosphatases are not correlated with CKa. The P values for the Null hypothesis of no correlation with CKa are: MGG_00149 P=2.7E-10, MGG_03154 P=2.5E-8, MGG_06099 P=4.0E-6, MGG_10195 P=6.9E-4, MGG_03838 P=8.8E-4, MGG_01690 P=2.6E-2

Transcriptomic data was downloaded from public websites so as to be able to test the relationship under many different growth conditions in many experiments.

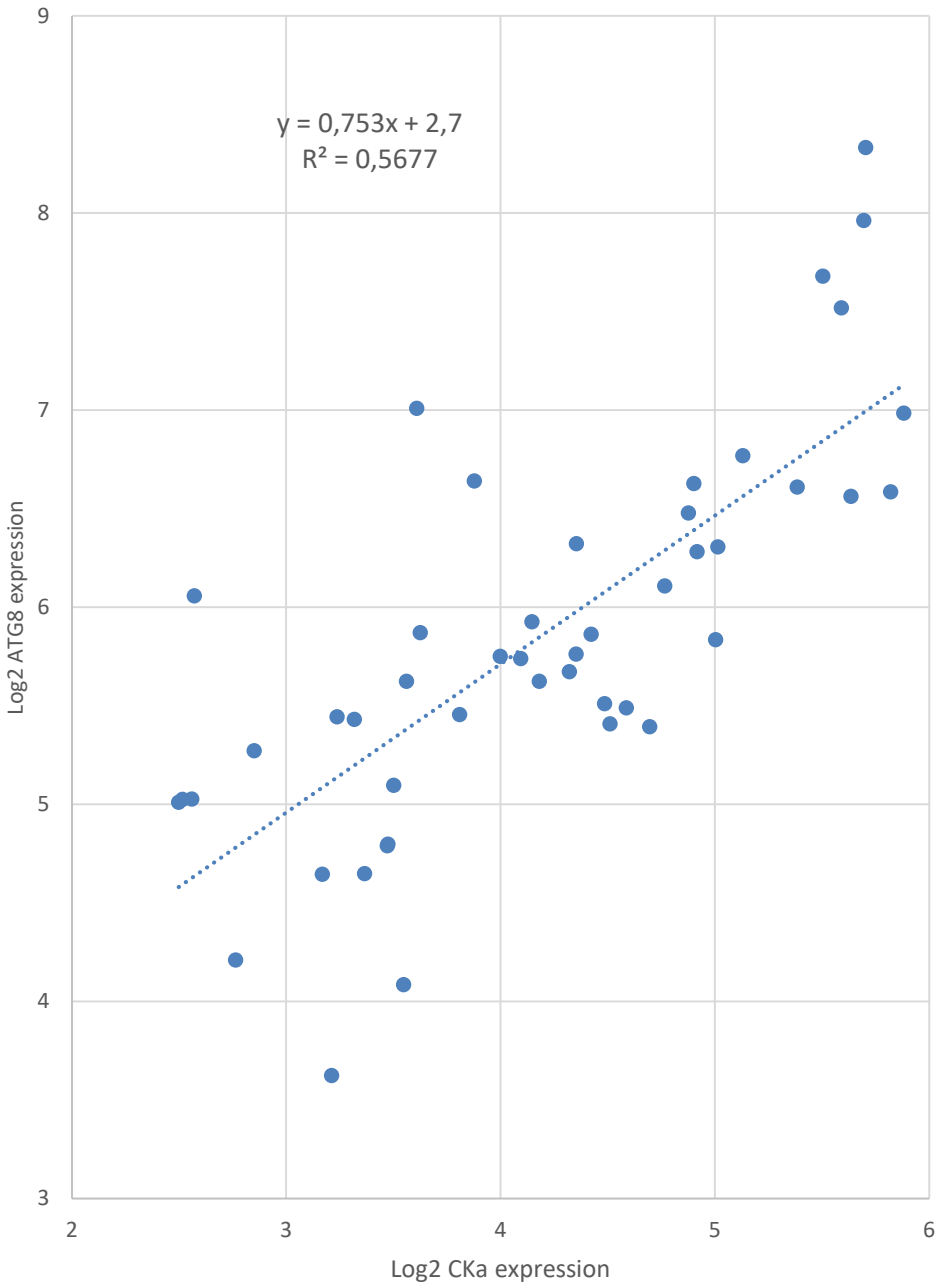

Figure 10 Plot of MoAtg8 (autophagy) expression vs MoCKa expression in a range of transcriptomes from different experiments (Note: Log2 scale on axes and grids are represented with fixed "aspect ratio“ to highlight the slope of the correlation). P value for the Null hypothesis that there is no correlation = 9.9E-10. Transcriptomic data was downloaded from public websites so as to be able to test the relationship under many different growth conditions in many experiments.

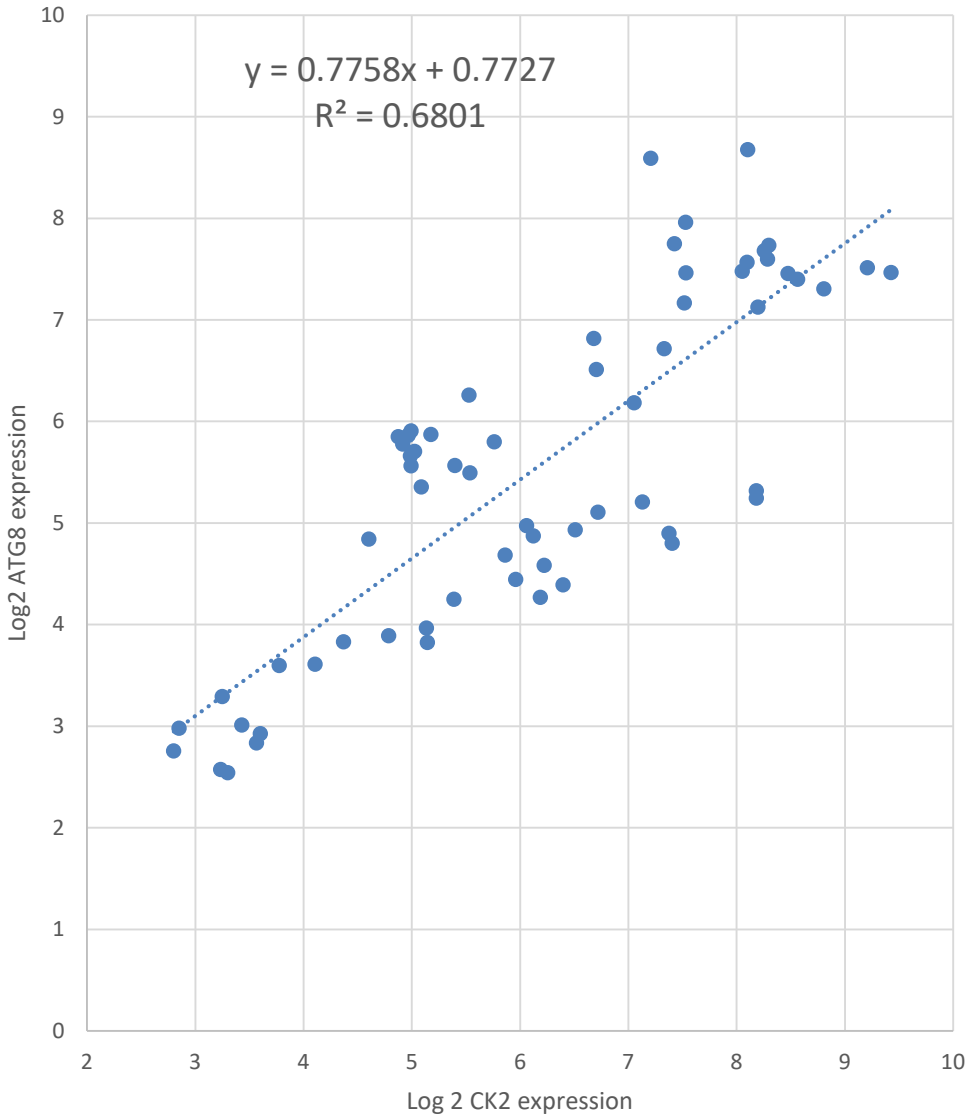

Figure 10 Supplement1. Plot of FgAtg8 (autophagy) expression vs FgCKa expression in a range of transcriptomes from different experiments. (Note: Log2 scale on axes and grids are represented with fixed "aspect ratio“ to highlight the slope of the correlation). P value for the Null hypothesis that there is no correlation = 5.5E-17. Transcriptomic data was downloaded from public websites so as to be able to test the relationship under many different growth conditions in many experiments.

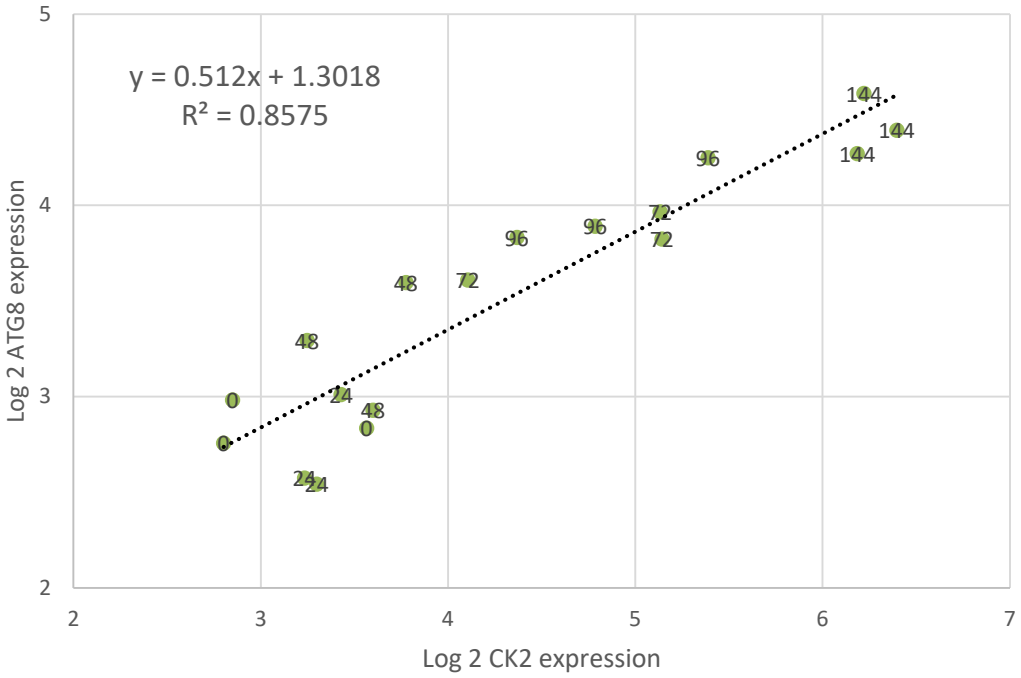

Figure 10 Supplement 2. Plot of FgAtg8 (autophagy) expression vs FgCKa expression in a times series infection experiment with 3 replicates where numbers in the plot indicate hours post infection (hpi). (Note: Log2 scale on axes and grids are represented with fixed "aspect ratio" to highlight the slope of the correlation). P value for the Null hypothesis that there is no correlation = 3.6E-08 . Transcriptomic data was downloaded from public websites so as to be able to test the relationship under many different growth conditions in many experiments.

Table 1 Background and mutant strains of *M. oryzae* used in this study

Strains	Genotype description	Reference
Ku80	*ku80* deletion mutant of Guy11 (Background strain in this study)	35
ΔMockb1	*Mockb1* deletion mutant of *Ku80*	This study
ΔMockb2	*Mockb2* deletion mutant of *Ku80*	This study
Mockb1C	*ΔMockb1* transformed with the wild-type MoCKb1 protein	This study
Mockb2C	*ΔMockb2* transformed with the wild-type MoCKb2 protein	This study
53OE	*ΔMockb2* transformed with the over-expressed GFP-MoCKa fusion protein	This study
43OE	*ΔMockb1* transformed with the over-expressed GFP-MoCKa fusion protein	This study
54OE	*ΔMockb2* transformed with the over-expressed GFP-MoCKb1 fusion protein	This study
45OE	*ΔMockb1* transformed with the over-expressed GFP-MoCKb2 fusion protein	This study
GFP-MoCKa	Ku80 transformed with the over-expressed GFP-MoCKa fusion protein	This study
GFP-MoCKb1	Ku80 transformed with the over-expressed GFP-MoCKb1 fusion protein	This study
GFP-MoCKb2	Ku80 transformed with the over-expressed GFP-MoCKb2 fusion protein	This study

Table 2 Primers used in this study

Primer name	The sequence of primer（5’→ 3’）
3696qRTF	CGTCAACTACCAGAAATGCG
3696qRTR	TGACGGAGTCTTGCTCTGTG
446qRTF	GCAGAGGTGTCGGAGGAAT
446qRTR	CCAAGATCATCTCCAGTGCC
5651qRTF	ACCCGTTGCTGCCGATGG
5651qRTR	TAGACCTGGAAGAGGATGTTGTGG
Tub1RTF	CAACATCCAGACCGCTCTC
Tub1RTR	ACCGACACGCTTGAACAG
446AF	GCCCAACCTTTCATCCTA
446AR	TTGACCTCCACTAGCTCCAGCCAAGCCTACCTCCAGTGCCTCCTT
446BF	GAATAGAGTAGATGCCGACCGCGGGTTCTCGTCCAACTCTAAACTAAC
446BR	GCTGGGTAAACATCTCATT
5651AF	GGGGTACCCCCTCTAAGTGGTCGTGC
5651AR	CCGGAATTCCTTGGATGGAATTGTGCC
5651BF	CGCGGATCCAGGGAGGCGTTATCATTTA
5651BR	TAATCTAGACAGAGCCGAGCTTGTCTA
446comF	GCTCTAGAGCGGAACCAGTAGTTGACGG
446comR	GGGGTACCCATGACAACGCCGGAGGG
5651comF	GCTCTAGAGCCCGACAAGCACAAAAGAT
5651comR	CCCCCGGGGAGCGTTCGTTTAGACCC
3696GFPF	CGGGATCCATGCACAGCATGGCACGC
3696GFPR	CGGAATTCTGTTGAAATTACCAGCGATTC
5651GFPF	CGGGATCCATGGAAGATTTTGGCAGCG
5651GFPR	CCCTCGAGTCAGACACCTTGCATCATG